PART II
DYNAMICAL MORPHOLOGY OF PROTON AURORA AND ELECTRON AURORA SUBSTORMS AND PHENOMENOLOGICAL MODEL OF MAGNETOSPHERIC SUBSTORMS

3. Diurnal Movement of the Location of Proton Auroras and Electron Auroras

3.1. Space-time diagrams of proton auroras and electron auroras

From the records of meridian-scanning photometers, spatial distributions of auroral luminosity along the geomagnetic meridian were arranged as a function of local time, and the iso-intensity contour lines were drawn. These space-time diagrams of auroral luminosity give quantitative information about the dynamic behavior of proton auroras and electron auroras as shown by HIRASAWA and NAGATA (1972). Diagrams were given for H_β and OI 5577 Å emissions which are the typical emission lines in proton auroras and electron auroras, respectively.

Assuming the auroral average height to be 100 km, the zenith angle is converted to the horizontal distance from the zenith over the observation point (Syowa Station). This space-time diagram covers a wide range from 600 km north

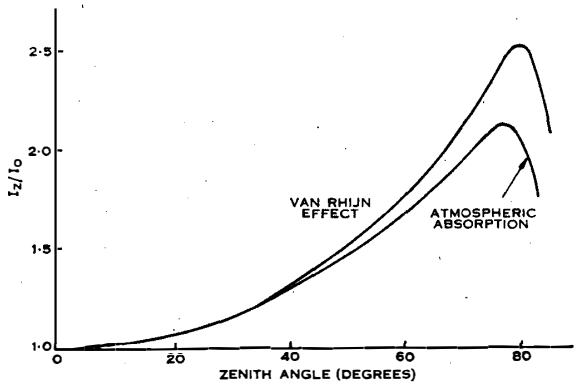

Fig. 15. Ratio of the intensity measured at a given zenith angle to that measured in the zenith, for an assumed thin uniformly emitting layer. A combination of the van Rhijn effect and atmospheric extinction results in an apparent enhancement of the emission with maximum intensity at a zenith angle of about 75° (after EATHER *and* JACKA, *1966).*

to 600 km south along the geomagnetic meridian. Numerals of the iso-intensity contour of H_β and OI 5577Å emissions are given in units of 8 R and 100 R, respectively.

Even if the actual emission is uniformly distributed, a scanning record across the sky shows an apparent enhancement of the emission with maximum intensity at a zenith angle of about 75° due to a combination of the van Rhijn effect and atmospheric extinction (EATHER and JACKA, 1966; Fig. 15). Since this apparent enhancement (by a factor of approximately two) of the emission near the horizon is not corrected in these space-time diagrams, it is necessary to note that the intensity increase by a factor of two near the horizon in the diagram is spurious. This remark is especially necessary for interpreting the diagram of H_β emission, because hydrogen emissions are more uniformly distributed over the sky than electron excited emission lines due to a charge exchange spreading of proton beam (DAVIDSON, 1965).

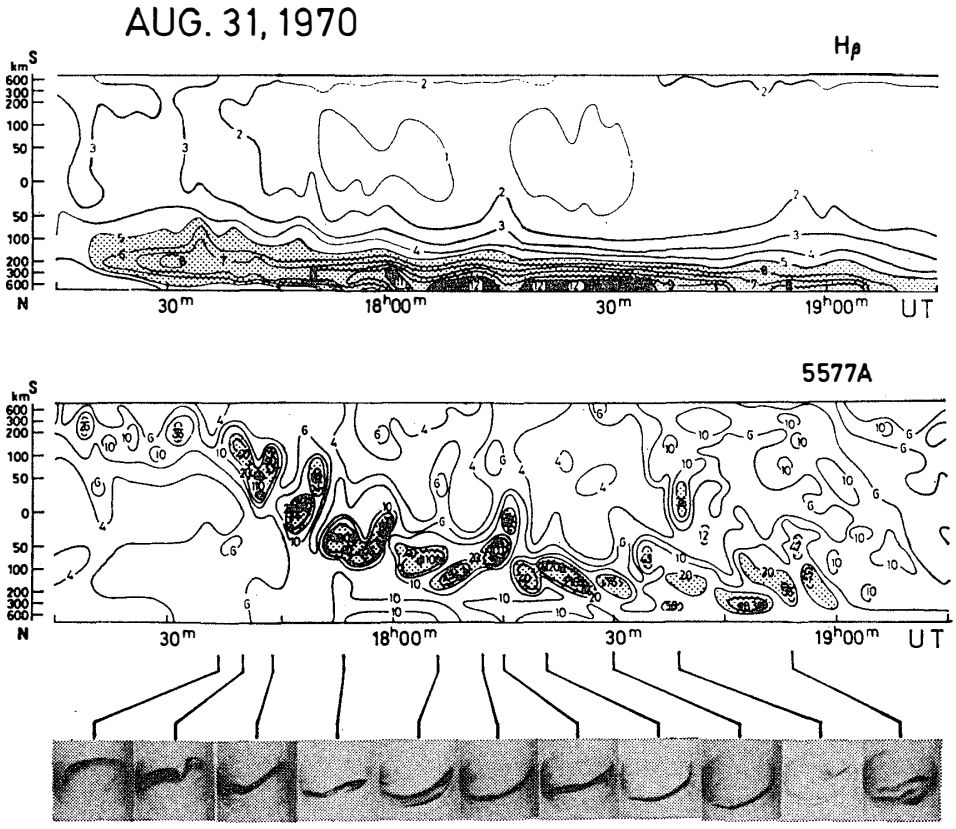

Fig. 16. Space-time diagram of H_β and OI 5577Å emissions and the simultaneous all-sky camera photographs on August 31, 1970. The hydrogen emissions are present on the equator-side of the active rayed bands of electron aurora. Numerals of the iso-intensity contours of H_β and OI 5577 emissions are given in units of 8 R and 100 R, respectively. Orientation of the all-sky camera photographs : top is the geomagnetic south (poleward) and left is the geomagnetic east.

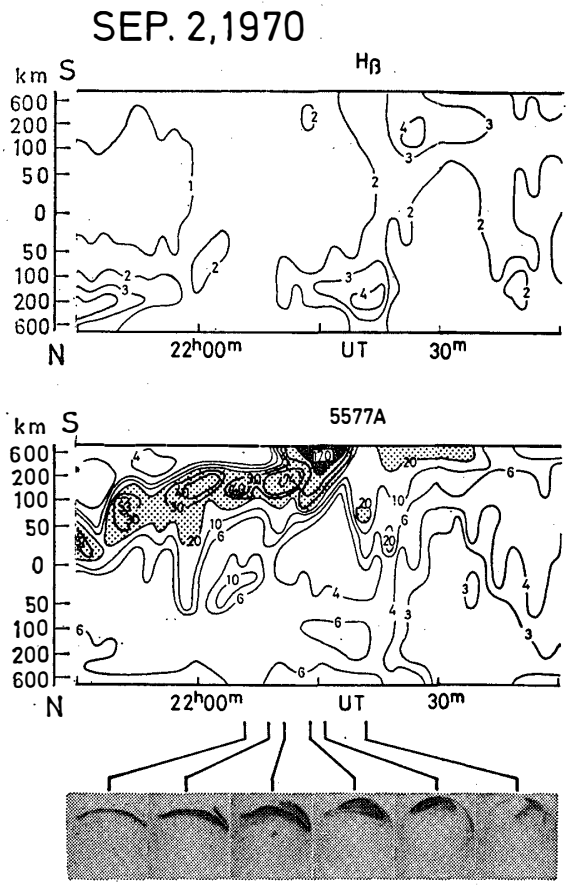

Fig. 17. Space-time diagram of H_β and OI 5577 emissions and the simultaneous all-sky camera photographs on September 2, 1970. The appearance of a westward traveling surge of the electron aurora at 2214 UT was followed by a rapid poleward expansion of the hydrogen emission zone. Orientation of the all-sky camera photographs: top is the geomagnetic south (poleward) and left is the geomagnetic west.

The examples of the space-time diagrams are shown in Figs. 16 and 17. In Fig. 16, the H_β emission zone is seen equatorward of an active rayed band of electron aurora. Fig. 17 is an example of the space-time diagram showing the appearance of a westward traveling surge of electron aurora near midnight and the following poleward expansion of the hydrogen emission zone.

3.2. Location of the emission regions of proton auroras and electron auroras on quiet days

Figs. 18 and 19 are examples of the space-time diagrams of H_β emission and OI 5577 emission on quiet days ($Kp \leq 2$). These diagrams show that the H_β emission is stationarily present from the evening to the morning with the intensity of 10 to 30R. The H_β emission zone is situated near the poleward horizon in the evening hours and it gradually moves equatorward before midnight and returns poleward after midnight, whereas the intensity of H_β emission remains fairly constant.

The intensity of OI 5577 emission is low (200–1000R), and its behavior is quite similar to that of H_β emission. This fact suggests that the greater part of

OI 5577 emission is excited by precipitating protons. Especially, in the evening hours the intensity ratio I (5577 Å)/I(H_β) is approximately 10, and this intensity ratio is in reasonable agreement with the theoretical prediction by EATHER (1967 a), if both OI 5577Å and H_β emissions are assumed to be simultaneously excited by precipitating protons. Therefore, the precipitating particles in this region are thought to be purely protons.

Geomagnetic latitude of Syowa Station is -66.7° and $L=6.4$, and the poleward horizon of Syowa Station (*i. e.*, 600 km south) is 72° lat. in geomagnetic coordinate and $L=10$. Therefore, the location of electron aurora oval is thought to be beyond the view of Syowa in the evening hours of quiet days. It is reasonable that proton auroras are observed in the evening hours without electron excited auroras. The location of the hydrogen emission zone on quiet days corresponds to the location of ring current protons in quiet times in the magnetosphere (FRANK, 1967b), suggesting that the source of proton auroras is ring current protons.

If the day before a quiet day is disturbed, the intensity of hydrogen emis-

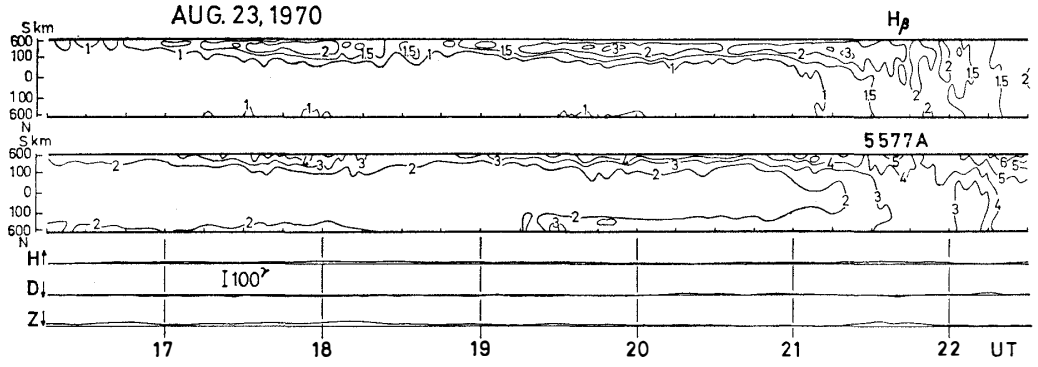

Fig. 18. Example of the space-time diagram of H_β and OI 5577 emissions in the evening hours on a quiet day, and the simultaneous record of geomagnetic variations.

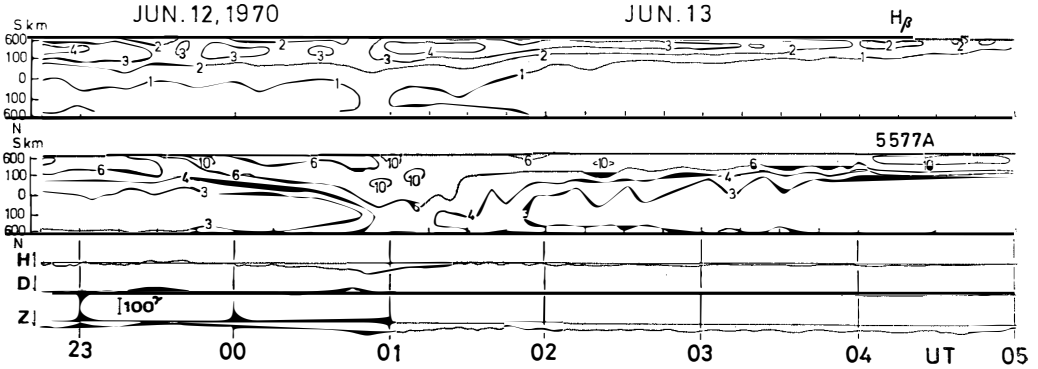

Fig. 19. Example of the space-time diagram of H_β and OI 5577 emissions in the midnight to morning hours on a quiet day, and the simultaneous record of geomagnetic variations.

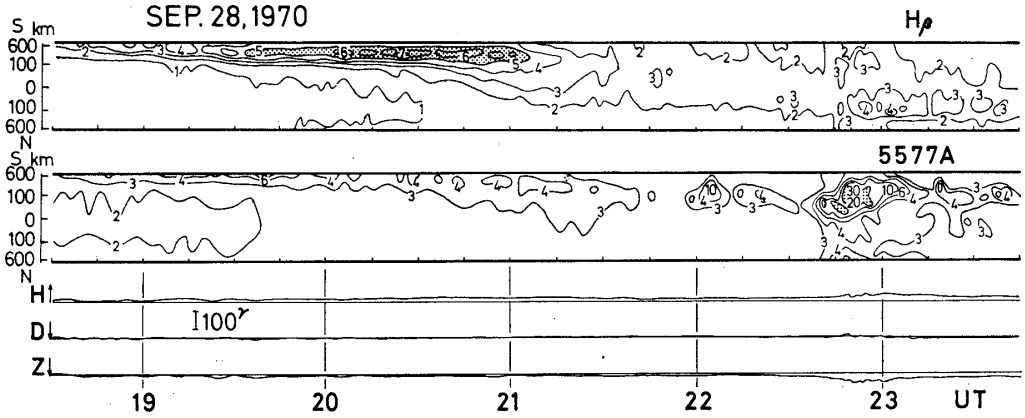

Fig. 20. Example of the space-time diagram of H_β and OI 5577 emissions on a quiet day. In contrast with the examples in Figs. 18 and 19, the previous day was disturbed ($\sum Kp=27$), and the increase in the hydrogen emission intensity in the evening hours is noticeable.

sions in the evening hours increases considerably, though the region of the emission is confined to the same location as the examples of Figs. 18 and 19 (Fig. 20). This fact indicates that the location of the emission zone of proton auroras depends on the configuration of the magnetic fields in the magnetosphere, but the intensity of the emissions depends on the total quantity of ring current protons which have been injected into the trapping region during the previous magnetospheric substorm.

In the midnight to morning hours, the intensity ratio I(5577 Å)/I(H_β) is about 20 – 30, and the behavior of OI 5577 emission in the space-time diagram is similar to that of H_β emission (Fig. 19). Therefore, it is concluded that electron auroras are present superimposed on hydrogen emissions in this local-time region on quiet days, *i. e.*, the emission zone of electron auroras (electron aurora oval) and the hydrogen emission zone overlap after midnight.

3.3. Location of the emission regions of proton auroras and electron auroras on disturbed days

On disturbed days when magnetospheric substorms develop, the behavior of proton auroras and electron auroras becomes quite active with rapid variations in both the location of the emission zone and the intensity. Fig. 21 is an example of the space-time diagrams of H_β emission and OI 5577 emission on a disturbed day. The most notable event in the H_β diagram is 1) a rapid equatorward movement of the hydrogen emission zone, which started about 2000 UT with a good correlation with the development of a positive bay, and 2) the rapid poleward expansion of the shifted emission zone after the onset of a negative bay at 2228 UT.

Apart from the OI 5577 emission excited by precipitating protons in the 5577 Å diagram through a comparison with the H_β diagram, the active OI 5577

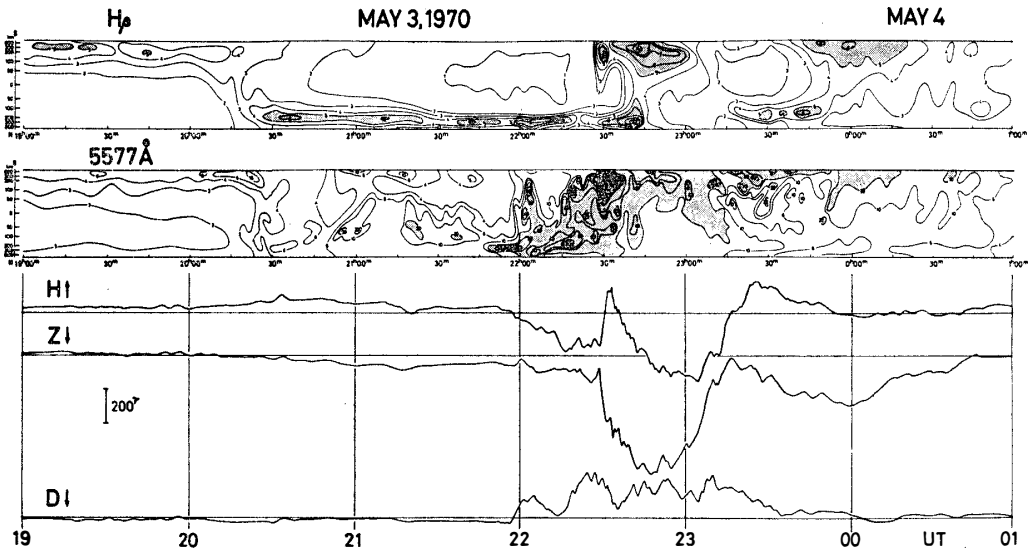

Fig. 21. Example of the H_β and OI 5577 emissions on a disturbed day, with the simultaneous record of geomagnetic variations.

emission excited by precipitating electrons appeared poleward of the equatorward-moving hydrogen emission zone, *i. e.*, in the void of the hydrogen emission. The breakup event of electron aurora occurred at 2156 UT, which is characterized in the 5577 Å diagram by a sudden increase of the intensity and the following rapid poleward motion resulting in the auroral bulge. At this time, however, the hydrogen emission zone did not expand poleward and remained near the equatorward horizon, suggesting that the breakup event of proton aurora and electron aurora does not start simultaneously in the same region. The equatorward shifted hydrogen emission zone returned poleward at the recovery phase of the last negative bay.

In the following chapter, the dynamic behavior of proton auroras and electron auroras in the course of magnetospheric substorms are studied in detail by using the space-time diagrams of H_β and OI 5577 emissions.

4. Dynamic Behavior of Proton Auroras and Electron Auroras during the Course of Magnetospheric Substorms

The dynamic behavior of proton auroras and electron auroras during a magnetospheric substorm greatly depends on the local time. First, proton aurora and electron aurora substorms observed in the late evening hours will be investigated. Geomagnetic local time (GLT) of Syowa Station is about 15 min later than universal time (UT).

4.1. Late evening hours (GLT 18–22 h)

In this interval, the most characteristic behavior of proton auroras is the rapid equatorward movement of the emission zone in the growth phase of a magnetospheric substorm. An example is shown in Fig. 22. The zone of the hydrogen emission started to move equatorward at approximately 1830 UT and the quiet arcs appear on the pole-side of the moving hydrogen emission zone. The intense surges of electron aurora traveled westward along the pre-existing arcs at 1940, 2040 and 2104 UT, respectively. After the appearance of a traveling surge, the location of quiet arcs returned poleward and then it moved equatorward again until the passing of a next traveling surge. The location of proton auroras, however, remained equatorward during the passing of a westward traveling surge in the evening hours. The intensity of the hydrogen emission began to increase about 20 min earlier than the first appearance of a traveling surge at 1940 UT.

Fig. 23 is the same example showing the equatorward movement of the hydrogen emission zone followed by a traveling surge of electron aurora on the pole-side of the hydrogen emission zone. The simultaneous records of the geomagnetic variations observed at the auroral-zone stations suggest that this rapid equatorward shift of the hydrogen zone is accompanied by the development of a positive bay in the evening hours.

As a measure of the worldwide development of polar magnetic substorms, AU and AL indices, introduced by DAVIS and SUGIURA (1966), were calculated

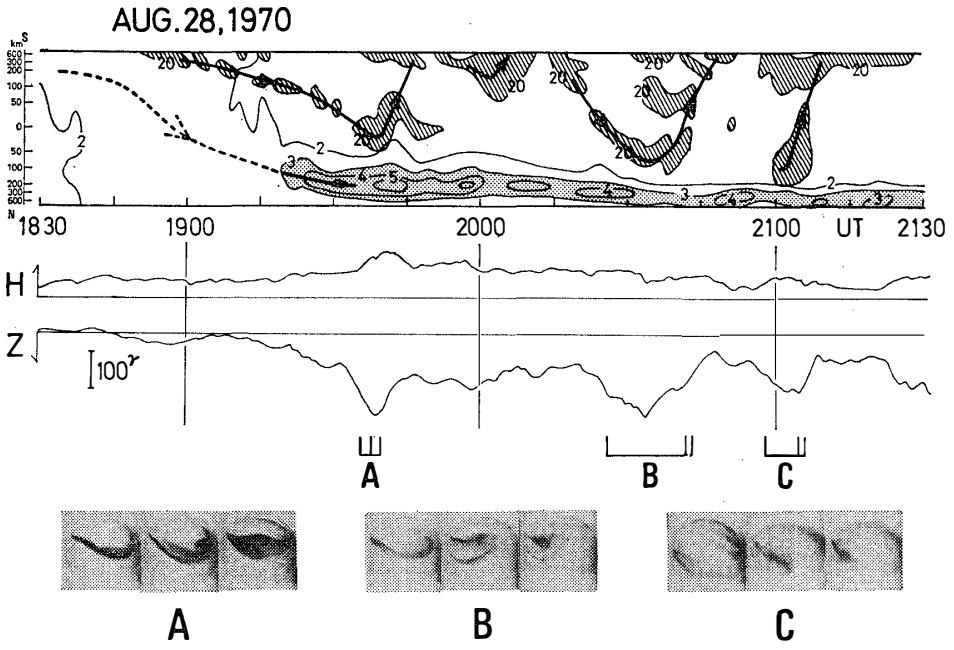

Fig. 22. Space-time diagram of H_β and OI 5577 emissions on August 28, 1970, with the simultaneous records of the geomagnetic H and Z components and the all-sky photographs. The H_β emission (proton aurora) is represented by the dotted areas, whereas the electron excited part in the OI 5577 emission, i. e., the electron aurora is indicated by hatched areas. The unit in the iso-intensity contour is the same as that in Figs. 16–21. The direction of the movement of proton and electron auroras is indicated by arrows. The top of the all-sky camera photographs is the geomagnetic south (poleward) and left is the geomagnetic west.

by superimposing the H-component values from a number of auroral-zone stations. The magnetograms of ten observatories were used ; Syowa Station, Mawson, Abisko, Dixon, Tixie Bay, Point Barrow, College, Fort Churchill, Great Whale River and Narsarssauq. AL is used as a measure of the intensity of westward electrojet in the midnight to early morning hours, whereas AU is used as a measure of eastward current in the noon to evening hours. Fig. 24 shows that the equatorward movement of the hydrogen emission zone which started at 2000 UT is simultaneously accompanied by the gradual growth of AL and AU. In this stage, the magnitude of AU is a little larger than the magnitude of AL, and the magnetic records from a number of polar magnetic stations indicate the growth of the bimodal DP-current field (DP 2). Therefore, this stage is defined as the growth phase of a magnetospheric substorm (IIJIMA and NAGATA, 1971).

Figs. 25a, b and 26a, b show also the close correlation between the rapid equatorward movement of the hydrogen emission zone and the gradual growth of AL and AU. The time intervals from the beginning of the equatorward movement to the onset of the expansion phase of a magnetospheric substorm was

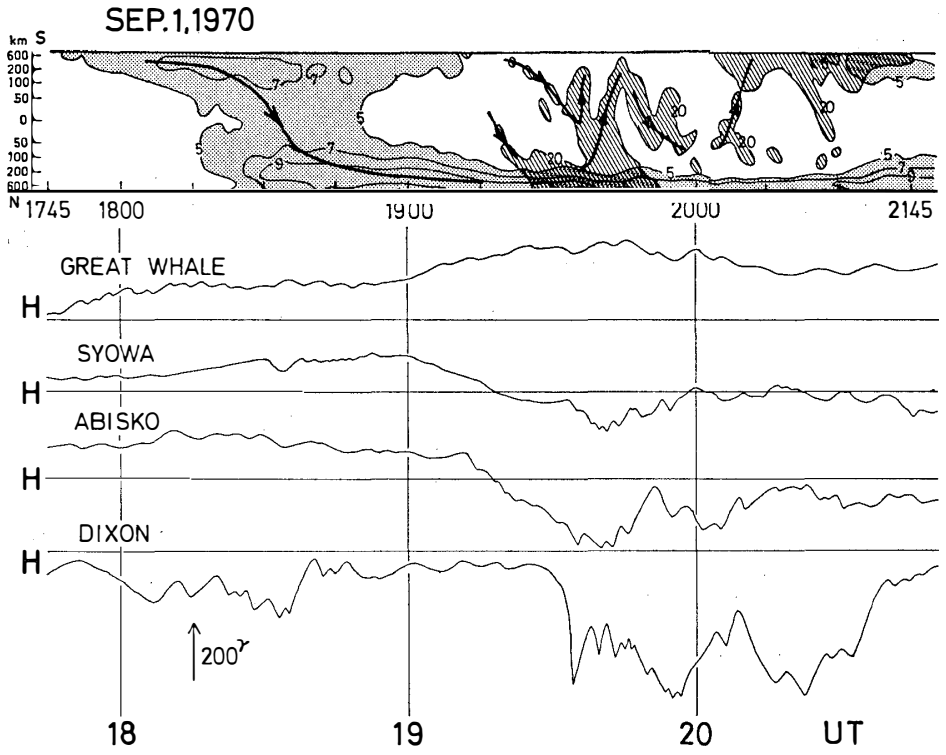

Fig. 23. Space-time diagram of H_β and OI 5577 emissions on September 1, 1970, with the simultaneous records of the geomagnetic H-component obtained at several auroral-zone stations. The notation in the space-time diagram is the same as that in Fig. 22.

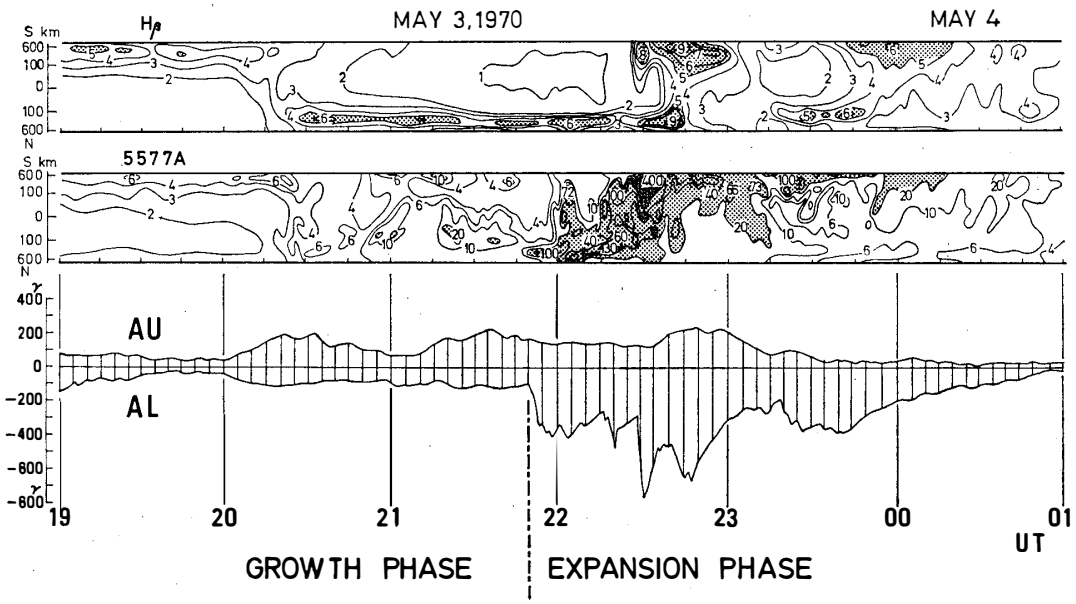

Fig. 24. Space-time diagram of H_β and OI 5577 emissions during the magnetospheric substorm on May 3, 1970, and the simultaneous AU and AL indices.

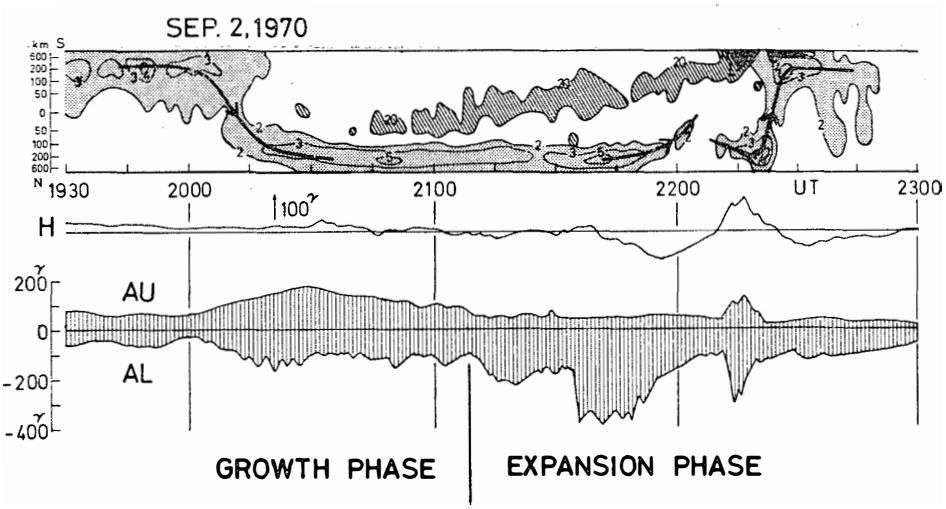

Fig. 25a. Space-time diagram of H_β and OI 5577 emissions during the magnetospheric substorm on September 2, 1970, and the simultaneous record of the geomagnetic H-component and AU and AL indices. The notation in the space-time diagram is the same as that in Fig. 22.

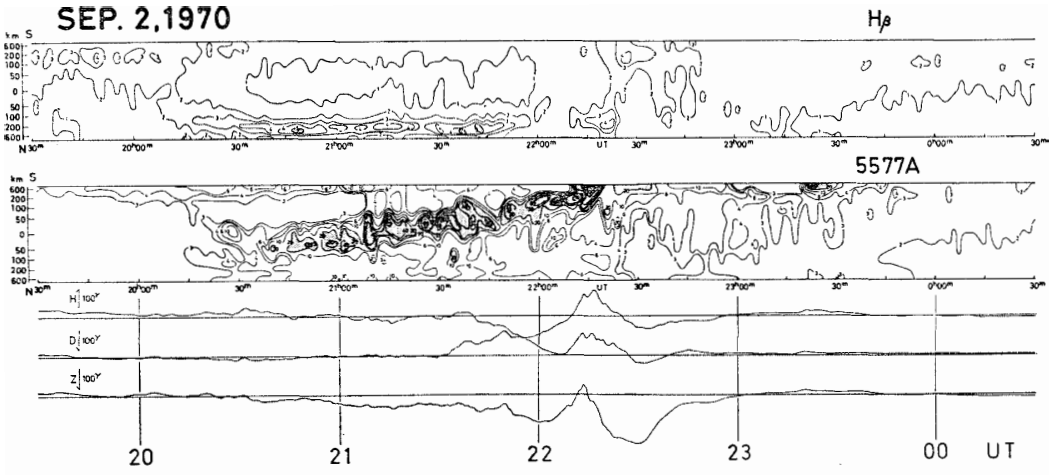

Fig. 25b. Original space-time diagram of H_β and OI 5577 emissions in Fig. 25a, with simultaneous record of the geomagnetic H, D and Z components.

approximately 70 and 30 min, respectively. These periods were fairly short compared with the period of the event of May 3, 1970 in Fig. 24, which was about 110 min.

During the expansion phase of a magnetospheric substorm which is characterized by a rapid increase of AL, the intense surges of electron aurora traveled westward on the pole-side of the hydrogen emission zone which remained near the equatorward horizon (Figs. 25a, b and 26a, b). This feature has already been mentioned in the events of Figs. 22 and 23. The shifted zone of hydrogen emis-

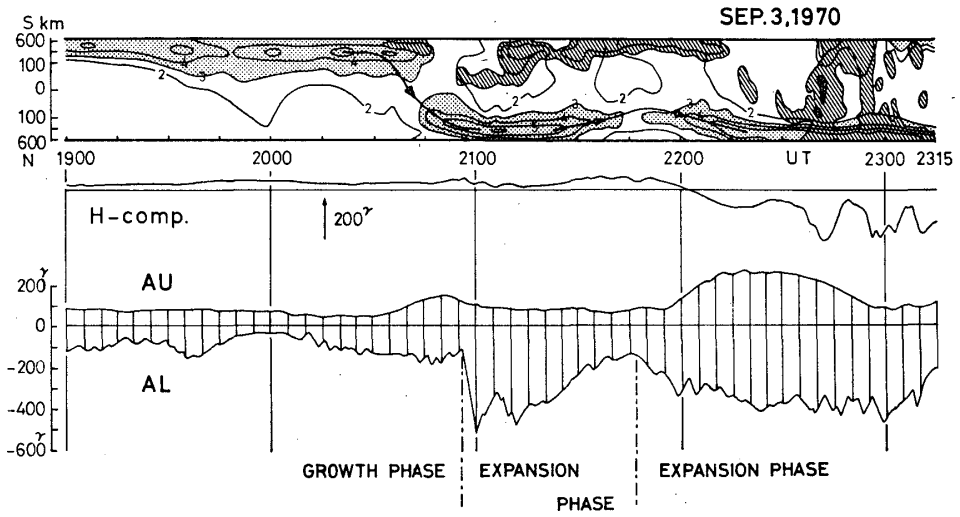

Fig. 26a. Space-time diagram of H_β and OI 5577 emissions during the magnetospheric substorm on September 3, 1970, and the simultaneous record of the geomagnetic H-component and AU and AL indices. The notation in the space-time diagram is the same as that in Fig. 22.

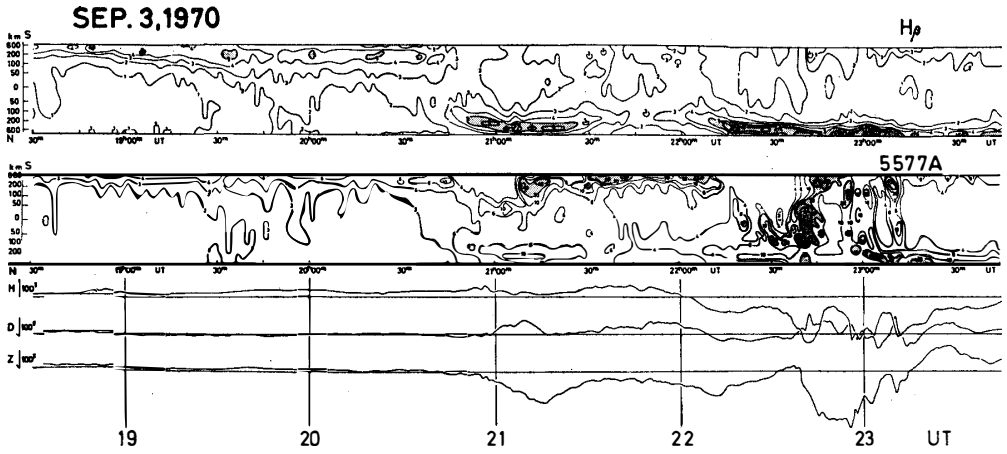

Fig. 26b. Original space-time diagram of H_β and OI 5577 emissions in Fig. 26a, with the simultaneous record of the geomagnetic H, D and Z components.

sion returned poleward in the recovery phase of a substorm (Figs. 26a, b).

Summarizing these results in the late evening hours, the equatorward movement of the hydrogen emission zone starts simultaneously with the onset of the growth phase of a magnetospheric substorm. The speed of the equatorward movement is strongly dependent on the local time with a maximum value of 250 m/sec at about 20 GLT (Fig. 27). Quiet arcs of electron auroras appear on the pole-side of the equatorward-moving hydrogen emission zone, and they also continue to move equatorward. In the expansion phase of a substorm, the intense surges

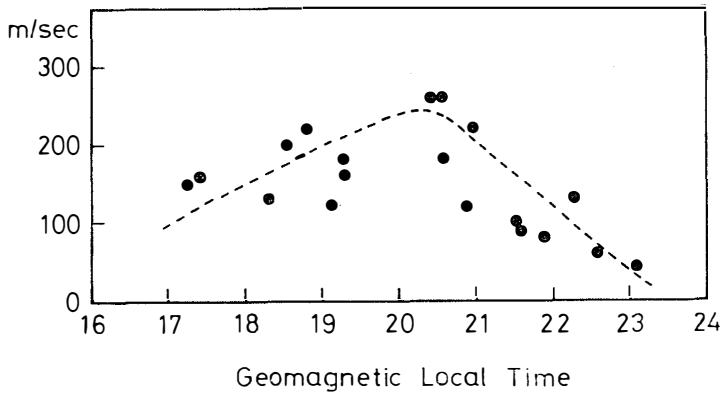

Fig 27. Speed of the equatorward movement of the hydrogen emission zone during the growth phase of a magnetospheric substorm as a function of the geomagnetic local time.

of electron aurora travel westward along the pre-existing arcs. Quiet arcs move equatorward before the passing of a westward traveling surge and return poleward after it, whereas the hydrogen emission zone remains near the equatorward horizon or continues to move equatorward with an increase in intensity. The poleward return of the hydrogen emission zone starts in the recovery phase of a substorm.

The equatorward movement of the hydrogen emission zone in the growth phase of a substorm is also closely correlated with the development of the asymmetric partial ring current in the evening region. This relationship is studied in detail in Chapter 5.

4.2. Late evening–midnight hours (GLT 22–00h)

The equatorward movement of the hydrogen emission zone during the growth phase is also observed in this local-time region, but the speed of the equatorward movement is slow as compared with the speed measured in the late evening hours (Fig. 27). At the onset of the expansion phase, one of the quiet arcs suddenly brightens and rapidly moves poleward and westward, resulting in the auroral bulge. A breakup event of the electron aurora is followed by a rapid poleward expansion of the hydrogen emission zone with a large increase of the intensity.

An example is shown in Fig. 28. Figs. 29a, b are another example which shows the gradual equatorward movement of the hydrogen emission zone before the onset of an intense negative bay at 2235 UT and the following rapid poleward expansion. The zone of hydrogen emission continued to move equatorward at the pre-breakup stage and resulted in a disappearance of the hydrogen emission between 2225 and 2235 UT due to the moving beyond the equatorward horizon of Syowa Station. After the onset of the first negative bay at 2235 UT, both proton aurora and electron aurora rappidly expanded poleward with a

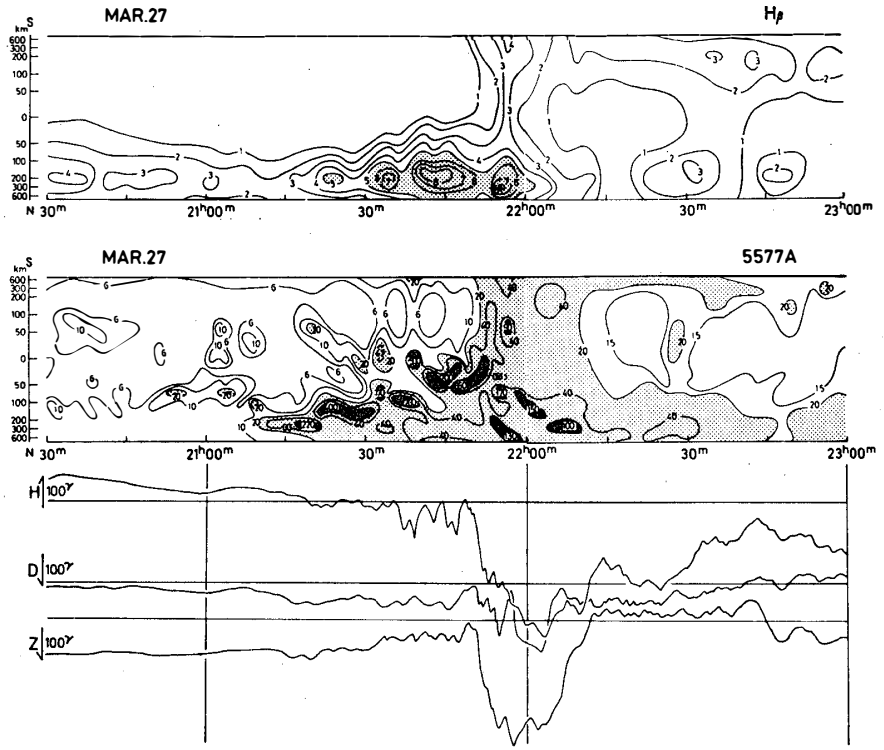

Fig. 28. Space-time diagrams of H_β and OI 5577 emissions on March 27, 1970, with the simultaneous record of the geomagnetic H, D and Z components. The breakup event of the electron aurora at 2148 UT was followed by the poleward expansion of the hydrogen emission.

sudden increase in the intensity of the emissions. However, a careful investigation of the breakup event in the space-time diagram shows the difference in the behavior of H_β emissions and OI 5577 emissions. This difference is notable during the second negative bay at 2248 UT. At this time, the hydrogen emission expanded poleward with a rapid increase in luminosity. Concerning the electron auroras, however, the intensity of arcs near the poleward horizon increased, but the definite breakup event was not seen from Syowa Station. The magnitude of the bay was larger in the geomagnetic Z component than in H component. These facts indicate that the breakup event of electron aurora was occurring beyond the poleward horizon. This dynamic relationship between proton auroras and electron auroras at the onset of a negative bay is confirmed by investigating the breakup event of electron aurora near the poleward horizon.

Figs. 30a, b illustrate that the negative bays started at 2132 and 2154 UT at Mowson (L=9.1) which is located poleward of Syowa Station (L=6.4). The onset of each negative bay was accompanied by a sudden brightening of electron aurora near the poleward horizon of Syowa Station. The movement of the hydrogen emission zone was equatorward before the onset of the first negative bay

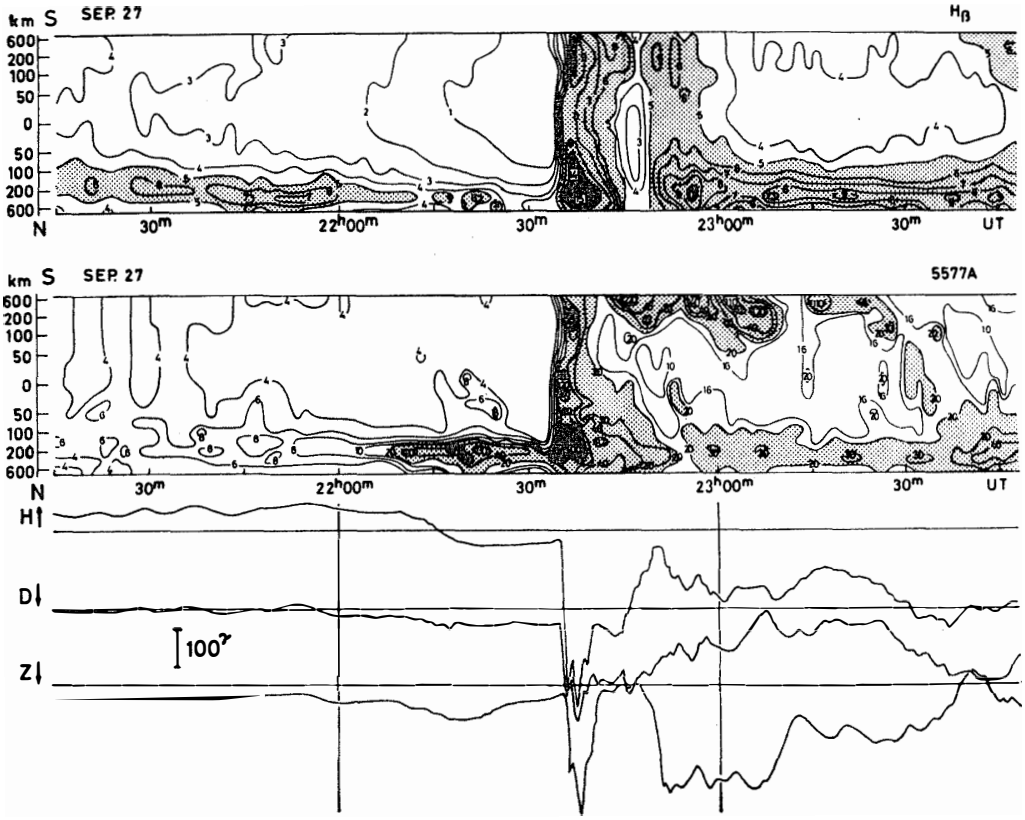

Fig. 29a. Example of the space-time diagram of H_β and OI 5577 emissions at the onset of a sharp negative bay near midnight, with the simultaneous record of the geomagnetic H, D and Z components.

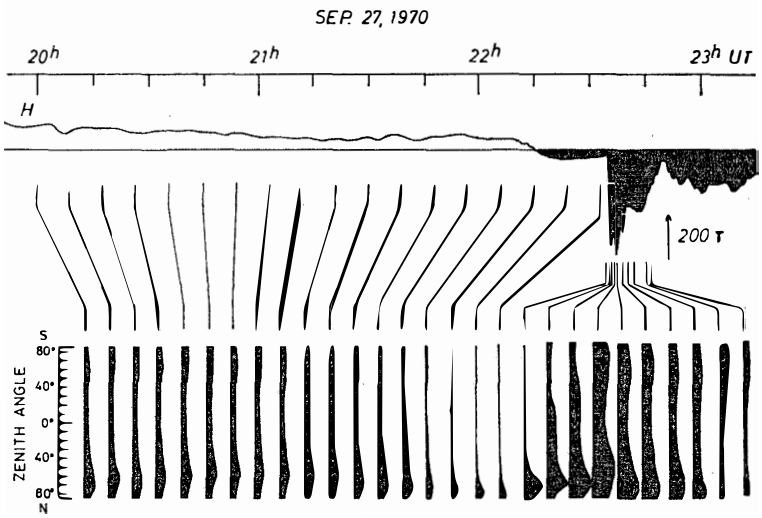

Fig. 29b. Time-variation in the intensity of H_β emissions along the geomagnetic meridian. The auroral space-time diagram in this interval is shown in Fig. 29a. The simultaneous record of the geomagnetic H-component is also illustrated (top), and the negative deviation from the quiet-time values is represented by shaded area.

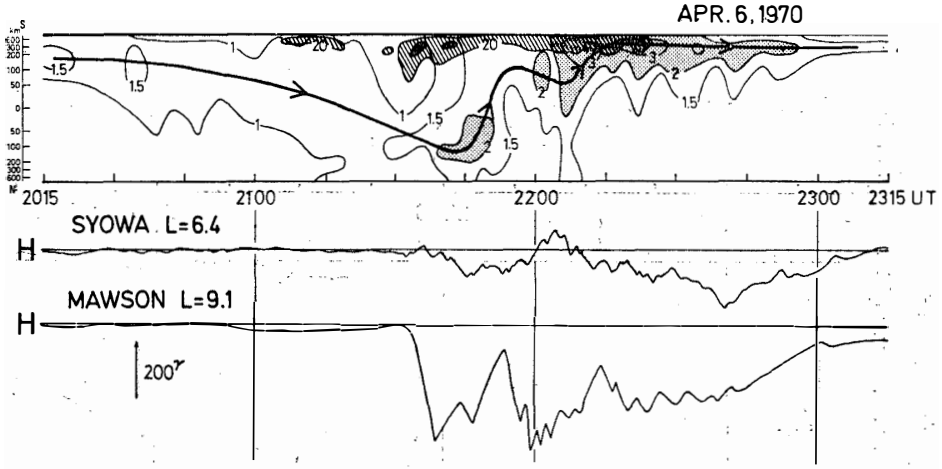

Fig. 30a. Space-time diagram of H_β and OI 5577 emissions on April 6, 1970, and the simultaneous records of the geomagnetic H-component obtained from Syowa Station and Mawson. The notation in the space-time diagram is the same as that in Fig. 22.

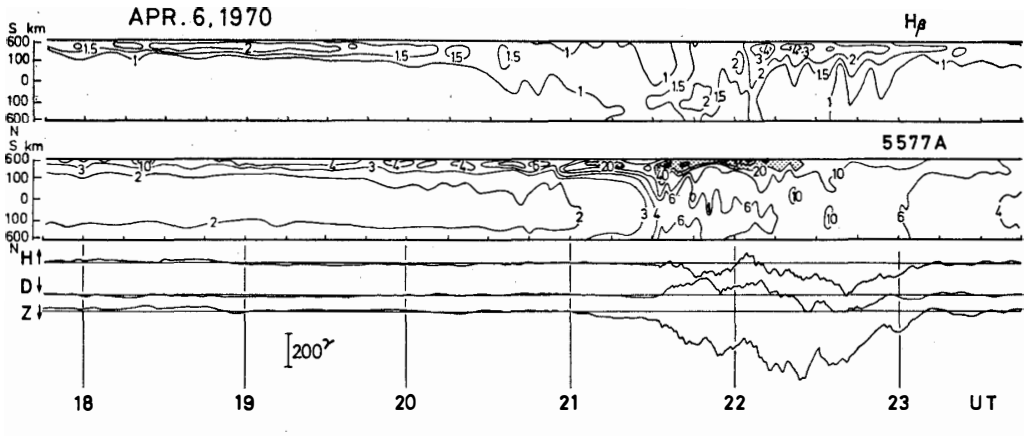

Fig. 30b. Original space-time diagram of H_β and OI 5577 emissions in Fig. 30a, with the simultaneous record of the geomagnetic H, D and Z components.

and was back poleward with an increase of the intensity as indicated by the arrows after the onset.

Figs. 31a, b are also typical examples of a electron auroral breakup event followed by the poleward expansion of the hydrogen emission. The equatorward movement of the hydrogen emission zone started at approximately 2115 UT with a gradual increase in AU and AL which suggests the development of the growth phase of a magnetospheric substorm. The expansion phase of a substorm started at 2200 UT and westward traveling surge passed by near the poleward horizon of Syowa Station at 2205 UT as illustrated with all-sky camera photographs. About 5 min after the passing of the traveling surge, the characteristic electron

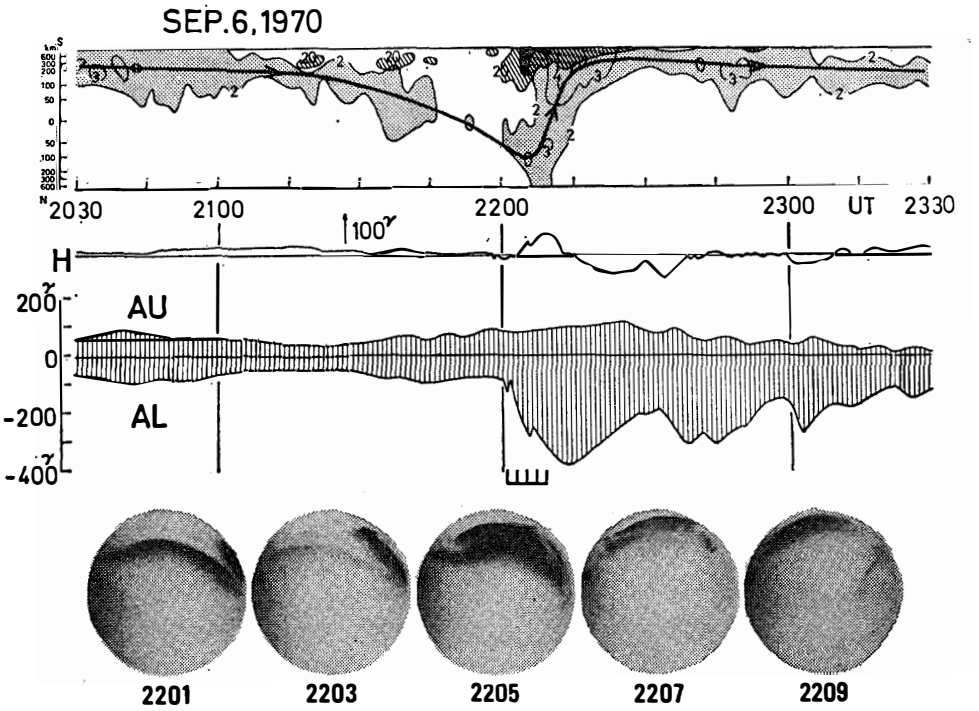

Fig. 31a. Space-time diagram of H_β and OI 5577 emissions on September 6, 1970, and the simultaneous record of the geomagnetic H-component, AU and AL indices and all-sky camera photographs. The notation in the space-time diagram is the same as that in Fig. 22.

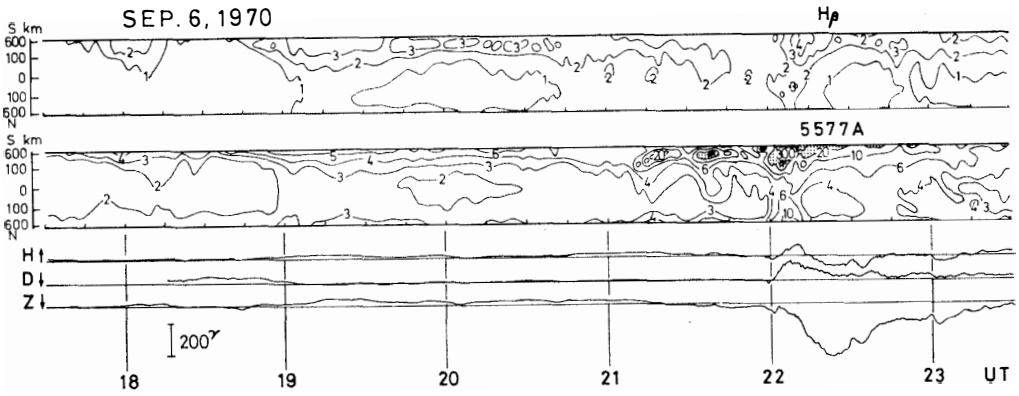

Fig. 31b. Original space-time diagram of H_β and OI 5577 emissions in Fig. 31a, with the simultaneous record of the geomagnetic H, D and Z components.

auroras called N–S oriented forms (MONTBRIAND, 1971) appeared and simultaneously the hydrogen emission zone started to move poleward with an increase in intensity. About 15 min after the onset of the expansion phase, the zone of hydrogen emission returned at the same location as that in the pre-growth phase.

A similar relationship between proton aurora and electron aurora is found at the breakup event of 2215 UT on September 2, 1970 in Figs. 25a, b. The all-sky camera photographs during the event are shown in Fig. 32. The photographs illustrate that N–S oriented forms appeared about 10 min after the passing of the westward traveling surge and were followed by a rapid poleward movement of the hydrogen emission zone. Summarizing these results, the relationship between the leading edge of the expanding electron auroral bulge and the hydrogen emission zone is schematically illustrated in Fig. 33.

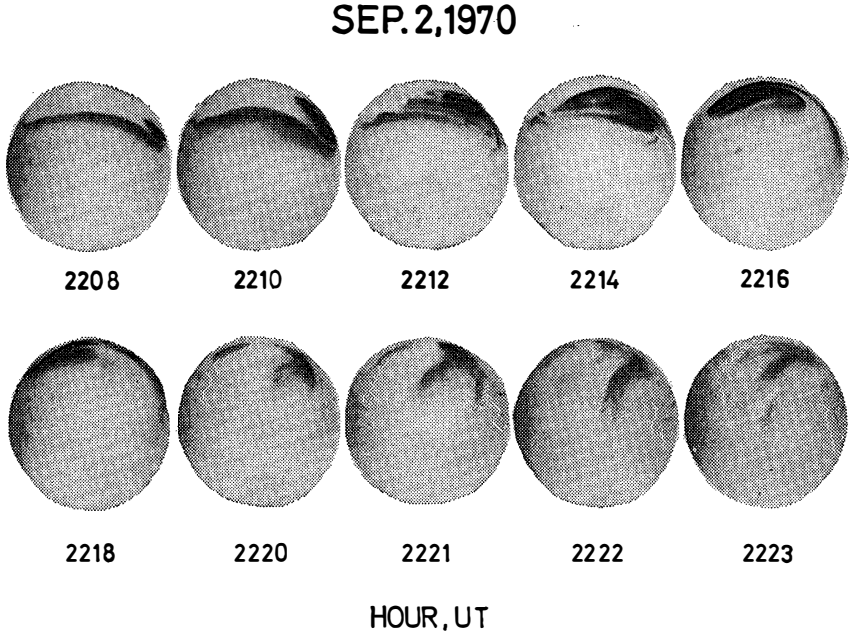

Fig. 32. All-sky camera photographs showing the passing of the westward traveling surge near the pole-side horizon and the subsequent appearance of the N–S oriented segments. The auroral space-time diagram during this event is illustrated in Figs. ***25a, b.***

Another example of the dynamic behavior of proton auroras and electron auroras in the late evening to midnight hours during a magnetospheric substorm is shown in Figs. 34a, b. With the gradual growth of AU and AL after 2000UT, the hydrogen emission zone started to move equatorward from the poleward horizon. Electron excited arcs appeared poleward of the moving hydrogen emission zone. The breakup event of electron aurora occurred three times at 2115, 2128 and 2140 UT. Each event was followed by the rapid poleward expansion of the hydrogen emission zone. After the last breakup event of electron aurora, the hydrogen emission zone returned to the poleward horizon, and diffuse electron auroras appeared on the equator-side of the hydrogen emission zone. The recovered hydrogen emission zone began to move equatorward again until the

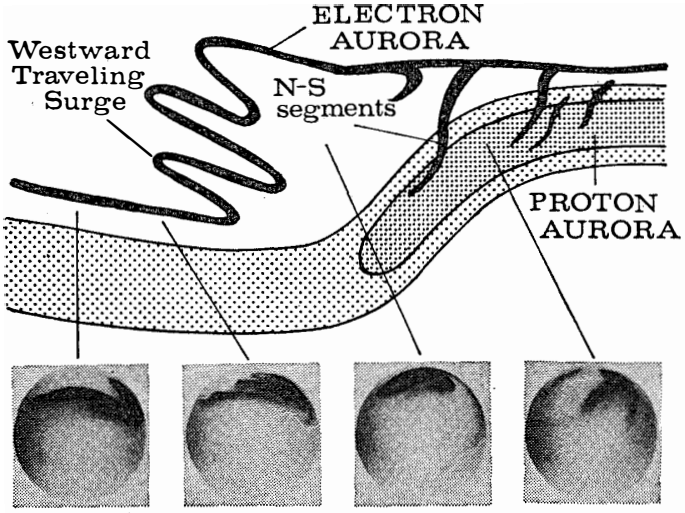

Fig. 33. Schematic diagram showing the relationship between the leading edge of an expanding electron aurora bulge and the hydrogen emission zone in the late evening to midnight region. The dense dotted area in the emission zone of proton auroras represents the region of enhanced hydrogen emission.

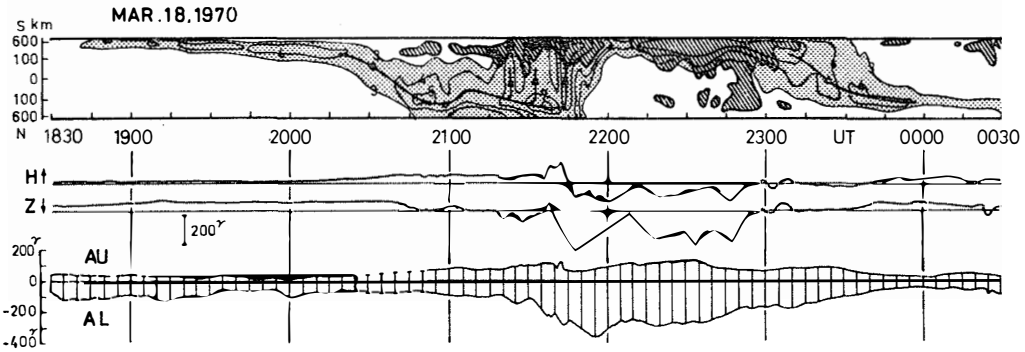

Fig. 34a. Space-time diagram of H_β and OI 5577 emissions during the geomagnetic substorm on March 18, 1970, and the simultaneous records of the geomagnetic H and Z components, and AU and AL indices.

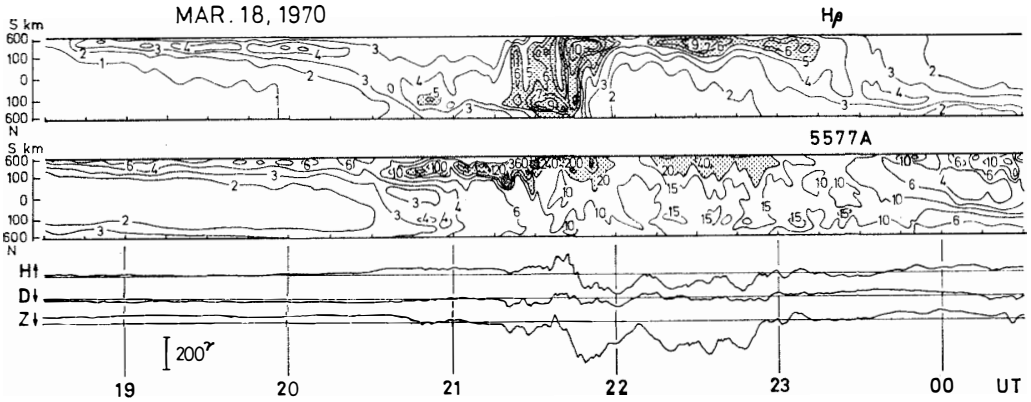

Fig. 34b. Original space-time diagram of H_β and OI 5577 emissions in Fig. 34a, with the simultaneous record of the geomagnetic H, D and Z components.

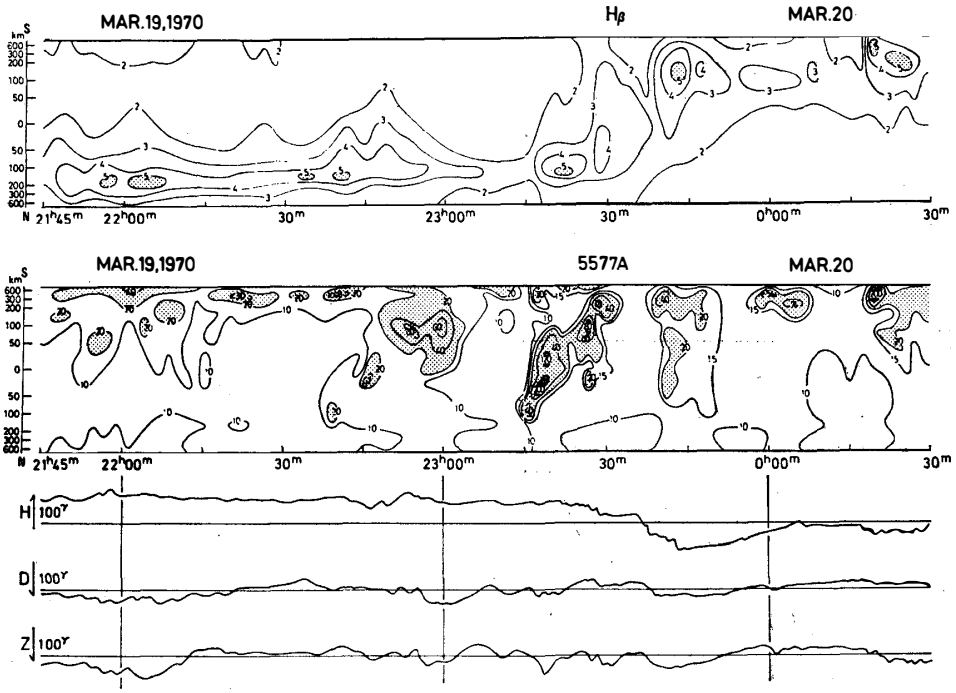

Fig. 35. Space-time diagram of H_β and OI 5577 emissions, with the simultaneous record of the geomagnetic H, D and Z components. The poleward return of the hydrogen emission zone is noticed after the breakup of an electron aurora at 2315 UT.

onset of the next expansion phase of a substorm. The poleward return of the hydrogen emission zone after the breakup of electron aurora is also distinctly shown in Fig. 35. That is, the most notable aspect of hydrogen emission behavior in the late evening to midnight hours is the gradual equatorward movement of the emission zone during the growth phase of a magnetospheric substorm and the rapid poleward return with an increase in the intensity during the following expansion phase.

4.3. Midnight–early morning hours (GLT 00–03h)

Concerning the auroras excited by precipitating electrons, active arcs or bands rarely appear from midnight to early morning, and faint diffused patches or rays are present equatorward of the hydrogen emission zone or superimposed on the diffuse hydrogen aurora. As to proton auroras, however, the intensity of the emission sometimes increases suddenly with a rapid poleward expansion of the emission zone during a gradual negative bay. Figs. 36a, b are examples of such an event. The rapid poleward movement of the hydrogen emission zone started at 0018 UT with a sudden increase in intensity. During the breakup event of the proton aurora, the breakup event of the electron aurora could not be seen from Syowa Station, but the weak rays excited by precipitating electron appeared near the zenith as shown by the all-sky photographs.

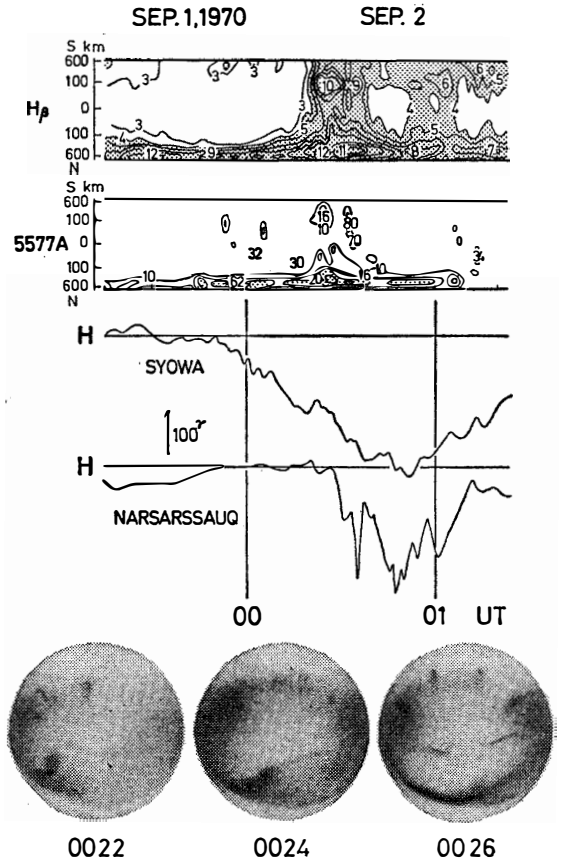

Fig. 36a. Space-time diagram of H_β and OI 5577 emissions, with the simultaneous records of the geomagnetic H-component obtained from Syowa Station and Narsarssauq. All-sky camera photographs taken at Syowa Station are also shown. Orientation of all-sky photographs: top is the geomagnetic south (pole-side), and left is the geomagnetic west.

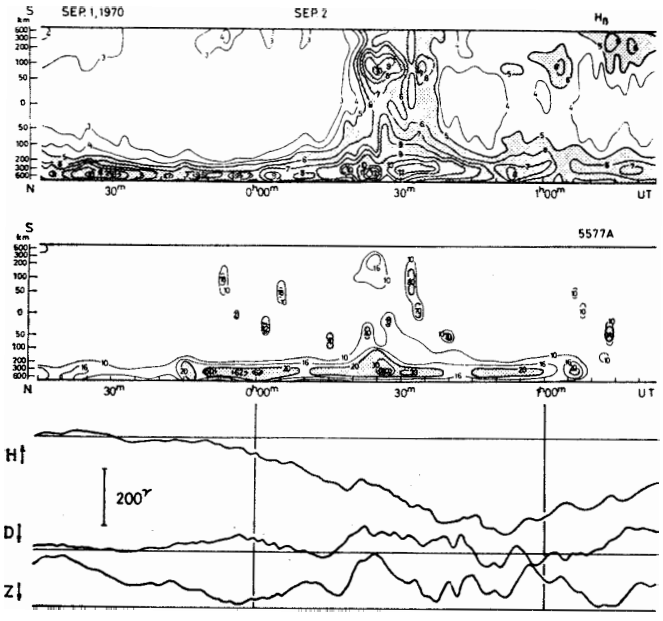

Fig. 36b. Original space-time diagram of H_β and OI 5577 emissions in Fig. 36a, with the simultaneous record of the geomagnetic H, D and Z components.

The H component of the geomagnetic variation at Syowa Station decreased gradually during this time, whereas a sudden decrease in the H component was observed at Narsarssauq, which is located in the pre-midnight region approximately 2 hours westward of Syowa Station. The onset of a sharp negative bay at Narsarssauq suggests that the breakup of the electron aurora occurred in this region.

It is concluded in Figs. 36a, b that a breakup event of proton auroras occurred in the post-midnight region simultaneously with the breakup event of electron excited auroras in the pre-midnight region. This relationship suggests that the mechanism for the auroral breakup accelerates electrons into the atmosphere in the pre-midnight region and protons in the post-midnight region, respectively.

After the last breakup event of proton auroras, the emission zone of proton auroras returns poleward, and diffuse patches or rays of electron auroras appear equatorward of the hydrogen emission zone or superimposed on the proton aurora.

4.4. Early evening hours (GLT 14–18h)

In this region, the electron auroral oval is located beyond the poleward horizon of Syowa Station except the period of an intense magnetic storm, whereas the hydrogen emission zone is situated equatorward of the electron aurora oval. Therefore, proton auroras are observed without accompanying electron auroras.

The emission zone of proton auroras moves gradually equatorward during the growth phase of a magnetospheric substorm, but the speed of the equatorward movement is slow as compared with that observed in the late evening hours (Fig. 27). Sometime after the onset of the expansion phase, the hydrogen emission zone expands equatorward with an increase in intensity. Fig. 37 is an example showing that the gradual equatorward movement of the hydrogen emission zone during the growth phase was followed by a rapid equatorward expansion after the onset of the expansion phase at 1853 UT. The expanded region of hydrogen emission contracted poleward toward the end of the recovery phase. The behavior of OI 5577 emission in the space-time diagram was quite similar to that of H_β emission suggesting that OI 5577 emission is excited by precipitating protons.

Another example is shown in Fig. 38. The hydrogen emission zone expanded equatorward with an increase in intensity sometime after the onsets of the expansion phase at 1624 and 1712 UT.

As shown in Figs 37 and 38, the development of the hydrogen emission has a good correlation with the development of a positive bay at Syowa Station. This fact suggests that the hydrogen emissions are closely related to the eastward electrojet. By using the magnetograms of Leirvogur, the conjugate station of Syowa, this relationship is studied further in detail. The sudden increase of AL at 1634 UT in Figs. 39a, b indicates the onset of the expansion phase of a substorm, and the preceding gradual development of AL and AU indicates the

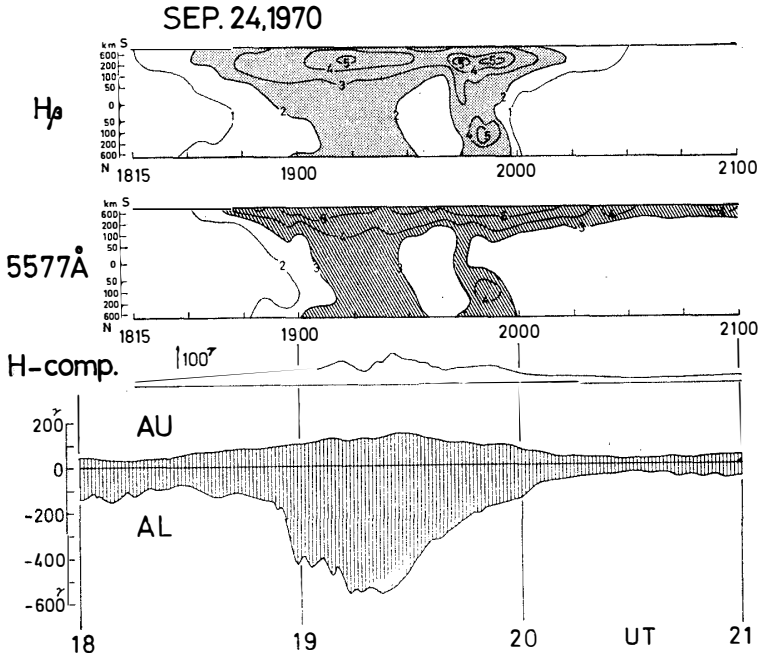

Fig. 37. Space-time diagram of H_β and OI 5577 emissions on September 24, 1970, and the simultaneous record of the geomagnetic H-component and AU and AL indices.

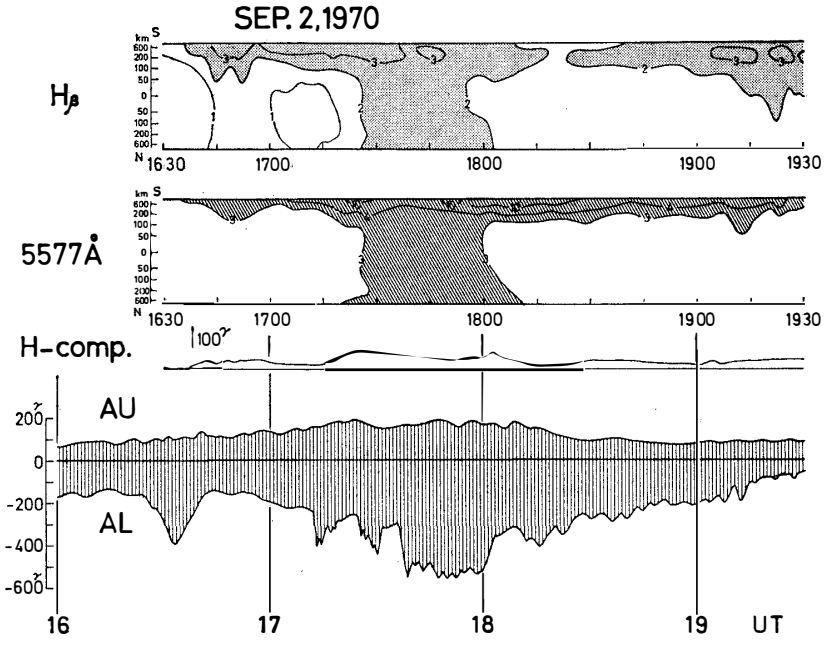

Fig. 38. Space-time diagram of H_β and OI 5577 emissions on September 2, 1970, and the simultaneous record of the geomagnetic H-component and AU and AL indices.

growth phase. The equatorward movement of the hydrogen emission zone with an increase of the intensity progressed during the expansion phase with a good correlation with a positive variation in H component at Syowa Station. The rapid increase in the intensity of hydrogen emission started at 1735 UT, namely about 1 hour after the onset of the expansion phase, and it was accompanied by

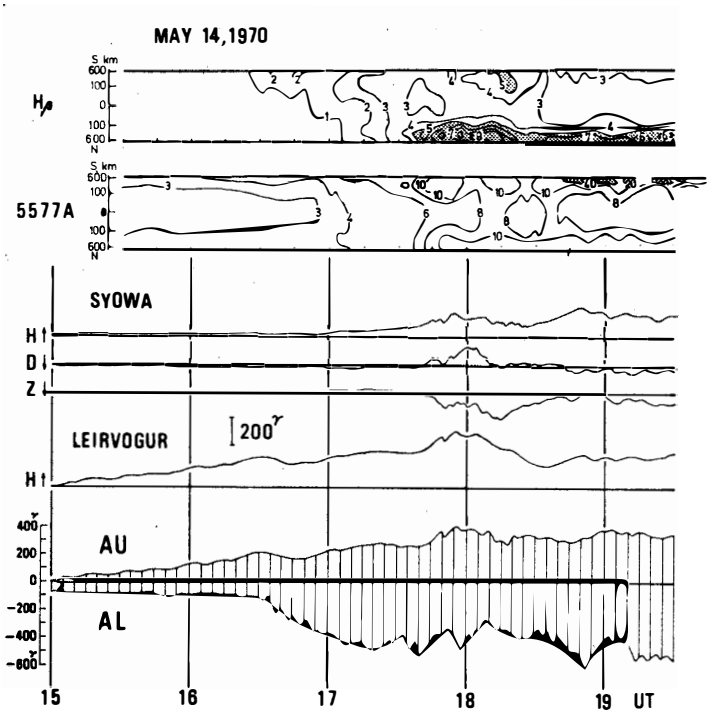

Fig. 39a. Space-time diagram of H_β and OI 5577 emissions, and the simultaneous records of the geomagnetic variations obtained from the conjugate-pair stations, i. e., Syowa Station and Leirvogur. AU and AL indices are also shown.

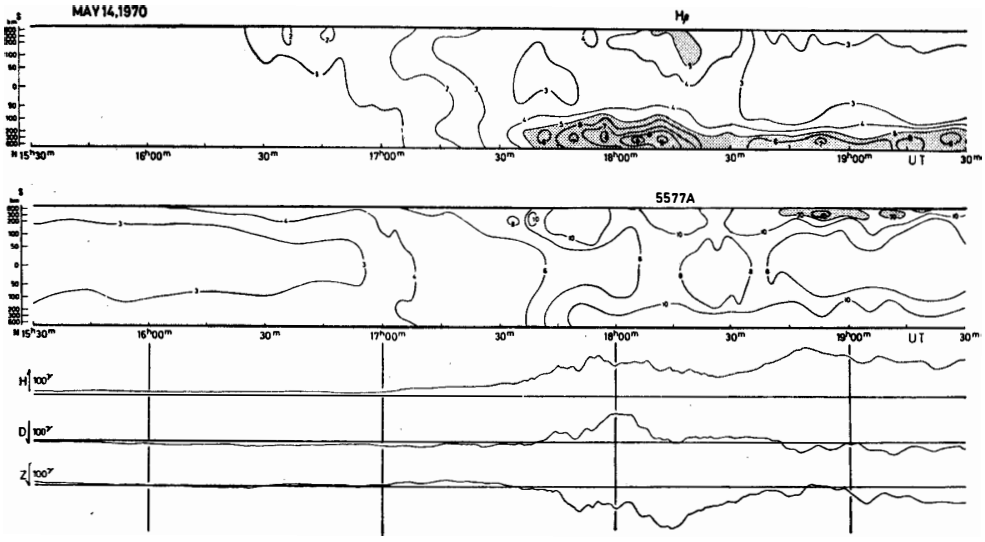

Fig. 39b. Original space-time diagram of H_β and OI 5577 emissions in Fig. 39a, with the simultaneous record of the geomagnetic H, D and Z components.

a large positive bay suggesting the development of the eastward electrojet. However, the H component of Leirvogur started to increase at 1500 UT, about 90 min before the onset of the expansion phase. The magnitude of the positive variation in H component at Leirvogur is much larger than that of Syowa Station.

This large asymmetry of H variation at the conjugate-pair stations is interpreted as implying that the positive variation of H component at Leirvogur before the development of an eastward electrojet is due to the intense bimodal DP-current (DP 2), whose magnitude shows a strong seasonal dependence, *i. e.*, the magnitude in the summer hemisphere is a few times that in the winter hemisphere (IIJIMA and NAGATA, 1971). In the event of May 14, 1970 in Figs. 39a, b, the positive H variation at Syowa Station in the winter hemisphere is thought to be mostly due to the eastward electrojet. A good correlation between hydrogen emissions and positive variation of geomagnetic H component suggests that the proton aurora is closely related to the generation of the eastward electrojet. This problem will be investigated in detail in Chapter 5.

5. Relationship between Proton Auroras, Positive Bays, Asymmetric Partial Ring Current and ULF Emissions in the Evening Hours

5.1. Relationship between proton auroras, high-latitude positive bays and asymmetric partial ring current in the evening hours

In this section, the simultaneous development of both proton auroras and positive bays in the evening hours during the course of a magnetospheric substorm is shown to be closely related to the development of an asymmetric partial ring current.

To measure the development of the ring current in the magnetosphere, the Dst-indices are usually used. The Dst is an average low-latitude geomagnetic disturbance field due to the ring current with respect to the geomagnetic dipole axis. However, the ring current is often thought to be asymmetric (AKASOFU and CHAPMAN, 1964; CUMMINGS *et al.*, 1968; FRANK, 1970). The DR-indices, introduced by KAMIDE and FUKUSHIMA (1971), are useful as a measure of the asymmetric partial ring current. These indices are derived from the geomagnetic H-component values at a number of stations of geomagnetic latitude 20°–40° distributed almost equally in longitude. DRS is the magnetic perturbation produced by a circular ring current at the equator on the earth's surface, whereas DRP is the magnetic perturbation produced by the westward partial ring current with a longitudinal width W centered at the local time T.

Using these DR-indices, we shall first study the relationship between proton auroras, positive bays and the asymmetric partial ring current during the expansion phase of a substorm. Fig. 40 is an example showing that the equatorward expansion of the hydrogen emission zone is closely correlated with the development of the positive bay and the asymmetric partial ring current, which are represented by AU- and DRP- indices, respectively. The development of the asymmetric partial ring current started at approximately 1825 UT with a gradual expansion of the hydrogen emission zone. The partial ring current intensity increased after the onset of the expansion phase at 1855UT, simultaneously with a rapid equatorward expansion of the emission zone. The center of the partial ring current simultaneously shifted westward from 18 h to 14 h GLT. On the other hand, the symmetric ring current intensity represented by DRS indices remained

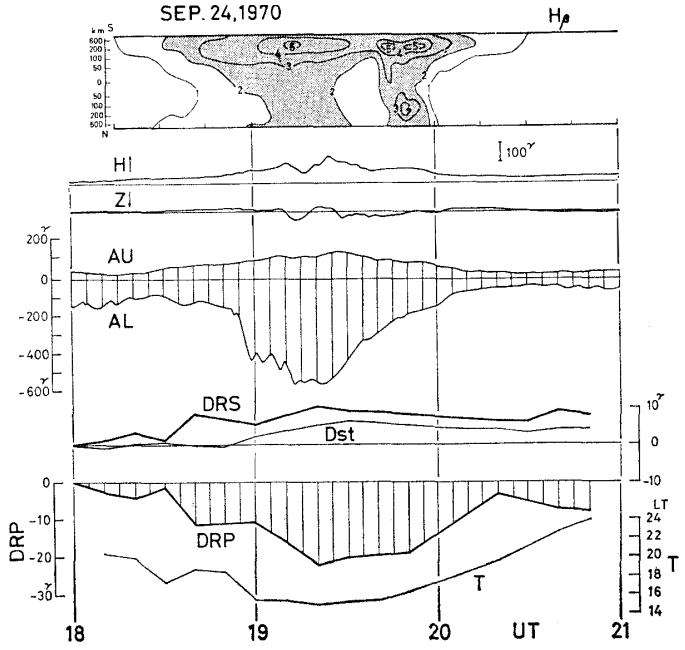

Fig. 40. Space-time diagram of H_β emission on September 24, 1970, with the simultaneous records of the geomagnetic H and Z components, and AE, Dst and DR indices. DRS represents a symmetric ring current intensity, while DRP index represents the intensity of an asymmetric partial ring current centered at local time T.

almost unchanged during this period. These facts suggest that the trapped protons, which have been injected into the trapping region on the midnight side at the expansion phase of a substorm, drift westward in the magnetosphere, producing the asymmetric partial ring current in the evening hours, and the protons precipitate into the ionosphere to excite the hydrogen emissions. That is, the source of the proton aurora in the evening hours during a magnetospheric substorm is thought to be the partial ring current protons.

Fig. 41 also illustrates how, after the onset of the expansion phase at 2150 UT, the intensity of the symmetric ring current (DRS) decreased while the asymmetric partial ring current (DRP) developed.

A close correlation between the proton aurora and the positive bay in Fig. 40 indicates that the positive bay is related to the increase in the ionospheric conductivity due to the proton precipitation. When the proton aurora shifts equatorward over the zenith at about 1910 UT, the deviation of the geomagnetic Z-component from the quiet-time values changes from minus to plus, suggesting that the positive bay in the evening hours is due to an eastward electrojet which flows in the zone of the hydrogen emission.

A definite correlation between proton auroras, positive bays and the asymmetric

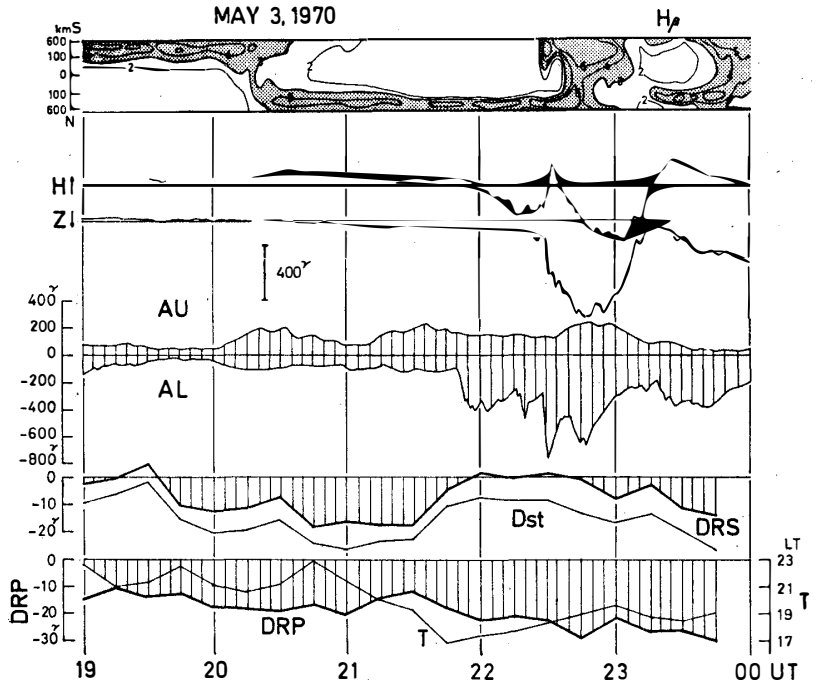

Fig. 41. Space-time diagram of H_β emission on May 3, 1970, with the simultaneous records of the geomagnetic H and Z components, and AE, Dst and DR indices.

partial ring current is also observed during the growth phase of a magnetospheric substorm. Fig. 41 shows that a rapid equatorward movement of the hydrogen emission zone during the growth phase before 2150 UT was accompanied by a large increase in both the symmetric ring current (DRS) and the asymmetric partial ring current (DRP). Since the source of proton auroras in the evening hours is thought to be ring current protons, the equatorward movement of the hydrogen emission zone corresponds to the earthward movement of the ring current protons in the magnetosphere. The marked correlation between the development of the ring current and the equatorward shift of the hydrogen emission zone is explained by the intensification of the ring current due to the rapid earthward drift of the ring current protons. The center of the partial ring current during the growth phase is located at the late evening region where the speed of the equatorward shift of the hydrogen emission zone is greatest. This fact suggests that the asymmetric partial ring current during the growth phase of a substorm is produced efficiently due to the very rapid earthward drift of the ring current protons in the late evening hours.

The positive variation of the geomagnetic H-component in the evening region during the growth phase of a magnetospheric substorm is thought to be due to the development of the bimodal DP current (IIJIMA and NAGATA, 1971). However, the precipitation of the ring current protons to the ionosphere results in an

increase of the ionospheric conductivity, producing a modification of the bimodal DP current. When the hydrogen emission zone moves equatorward over the zenith at about 2018 UT during the growth phase, the deviation of the geomagnetic Z-component from the quiet-time values, ΔZ, changes from minus to plus (Fig. 41), suggesting again that the eastward concentrated current flows in the hydrogen emission zone.

Fig. 42 is another example showing that the rapid equatorward movement of the hydrogen emission zone during the growth phase is accompanied by a development of the asymmetric partial ring current whose center is located in the late evening hours.

In the event of September 3, 1970 shown in Fig. 43, the time interval from the beginning of the equatorward shift of the hydrogen emission zone to the onset of the expansion phase at 2056 UT is short, and the relationship between the equatorward shift and the development of the ring current is obscure during the growth phase. In the expansion phase, however, it is noticeable that the equatorward movement of the hydrogen emission zone with increasing emission intensity is closely related to a development of the partial ring current, and the

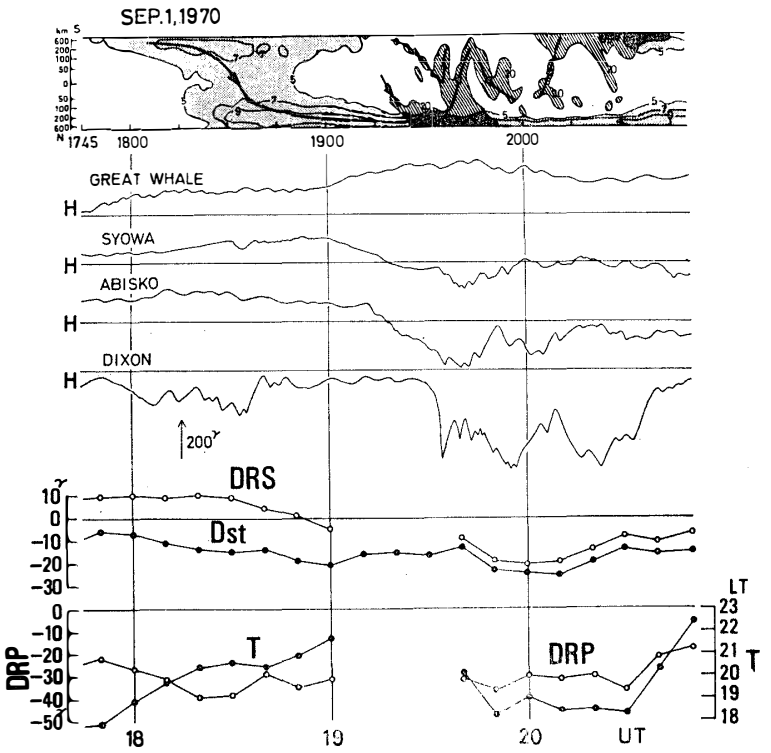

Fig. 42. Space-time diagram of H_β and OI 5577 emissions on September 1 1970, with the simultaneous records of the geomagnetic H component obtained from several auroral-zone station, and Dst and DR indices. The notation in the space-time diagram is the same as that in Fig. 22.

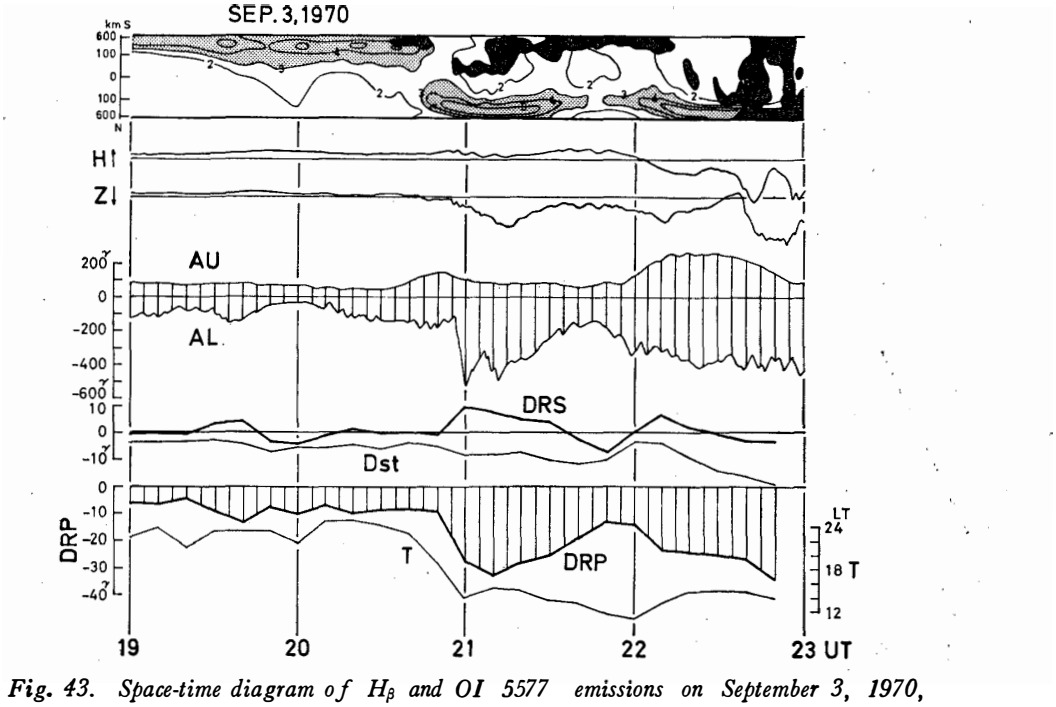

Fig. 43. Space-time diagram of H_β and OI 5577 emissions on September 3, 1970, with the simultaneous records of the geomagnetic H and Z components, and AE, Dst and DR indices. The notation in the auroral space-time diagram is the same as that in Fig. 22.

poleward movement of the emission zone is accompanied by a decrease in the intensity of the partial ring current.

The relationship between proton auroras, positive bays and the asymmetric partial ring current during a course of a magnetospheric substorm are summarized as follows. In the growth phase, the rapid equatorward movement of the hydrogen emission zone is accompanied by an increase in the intensity of both the symmetric ring current and the asymmetric partial ring current. The center of the partial ring current is located at the late evening region where the equatorward shift of the emission zone is greatest. During the expansion phase, however, the partial ring current greatly develops in the evening hours without an accompanying growth of the symmetric ring current. The development of the partial ring current is closely correlated with the equatorward expansion of the hydrogen emission zone and with an intense enhancement of the luminosity. The relationship between the movement of the hydrogen emission zone and the variation of the geomagnetic Z-component is such that when the emission zone moves over the zenith from the poleside, ΔZ (the deviation from the quiet-time values) changes from minus to plus, and vice versa. This relationship suggests that the eastward concentrated current is present in the hydrogen emission zone, not only in the expansion phase but also in the growth phase of a substorm.

5.2. Relationship between proton auroras, cosmic noise absorption and ULF emissions (IPDP) in the evening hours

IPDP events are a particular type of geomagnetic micropulsations with rising mid-frequencies, observed in the evening hours during positive bays. This event is thought to be generated by the ion cyclotron resonance mechanism (HEACOCK, 1967; MCPHERRON *et al.*, 1968; FUKUNISHI, 1969; GULYEL'MI *et al.*, 1970; GENDRIN, 1970). FUKUNISHI (1969) suggested that ring current protons impulsively injected into the trapping region near midnight at the onset of the expansion phase of a magnetospheric substorm drift westward, exciting IPDP events. The rising of the mid-frequency of IPDP was explained by the earlier arrival of higher-energy protons followed by lower-energy protons over a given recording site; the pulsation frequency varies with energy in the proportion $f \sim 1/E^{\frac{1}{2}}$. If the IPDP events are generated by the ion cyclotron resonance mechanism, the excited ion cyclotron waves will cause a pitch-angle diffusion loss of protons from the magnetosphere into the ionosphere. Therefore, the appearance of the proton aurora is expected

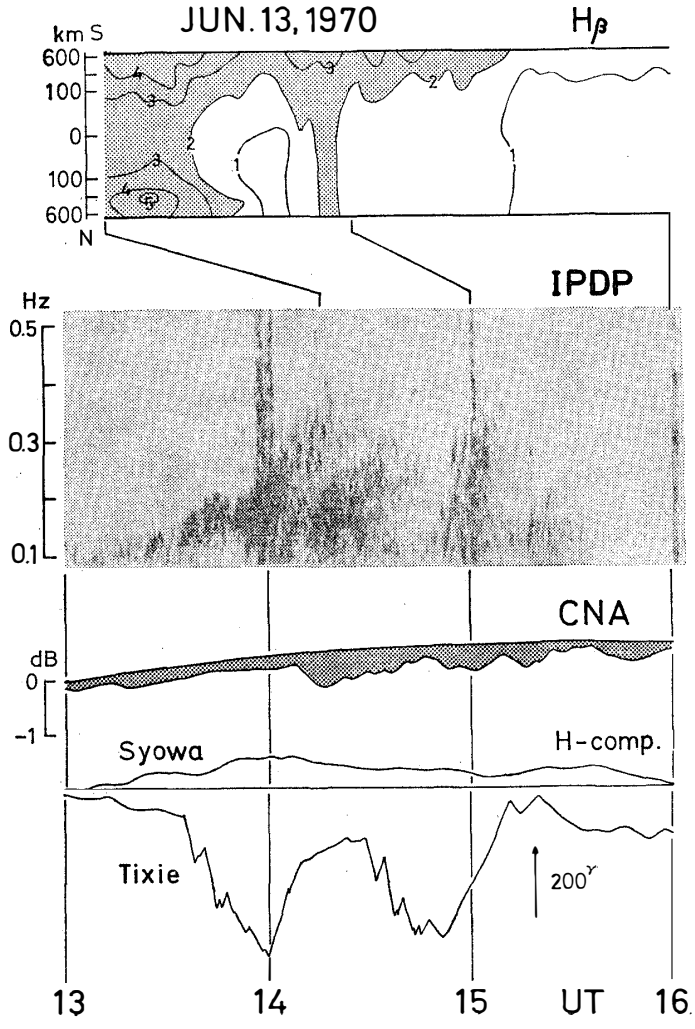

Fig. 44. Example of the relationship between proton aurora, IPDP event, cosmic noise absorption and positive bay in the early evening hours. Top: space-time diagram of H_β emission; middle: sonagram of the geomagnetic micropulsation and record of 30 MHz cosmic noise absorption; bottom: records of the geomagnetic H component obtained from Syowa Station in the evening region and Tixie near midnight.

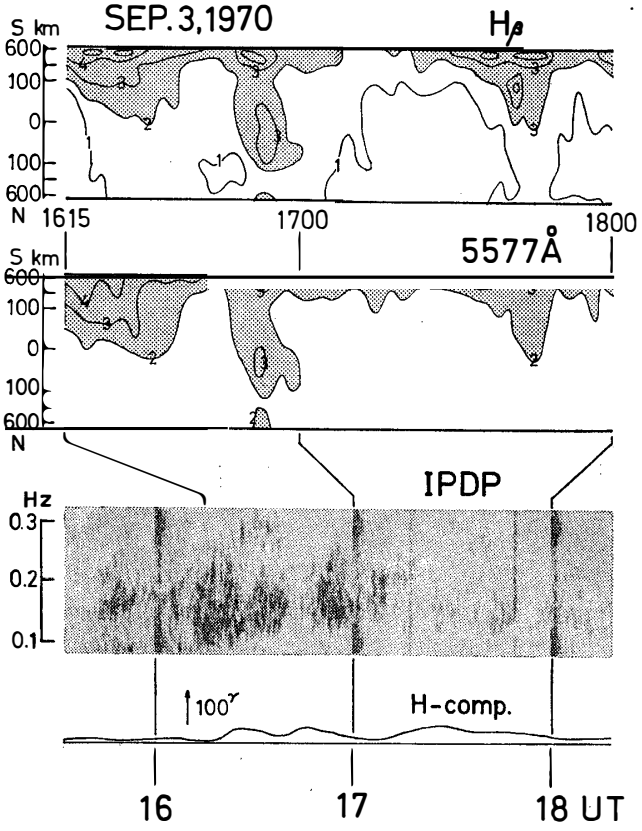

Fig. 45. Example of the relationship between proton aurora, IPDP event and a positive bay in the early evening hours. Top: space-time diagrams of H_β and OI 5577 emissions; middle: sonagram of the geomagnetic pulsation; bottom: record of the geomagnetic H component.

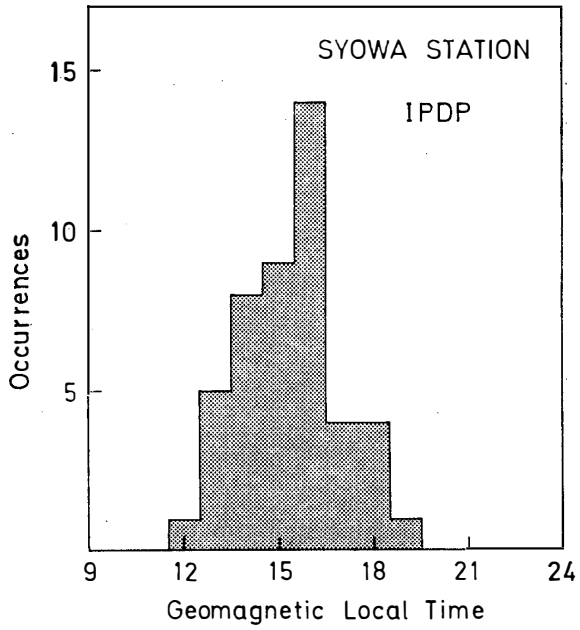

Fig. 46. Diurnal variation in occurrences of IPDP events observed from March to September, 1967 at Syowa Station.

during the IPDP event. Figs. 44 and 45 are examples showing a good correlation of the proton auroras and the IPDP events.

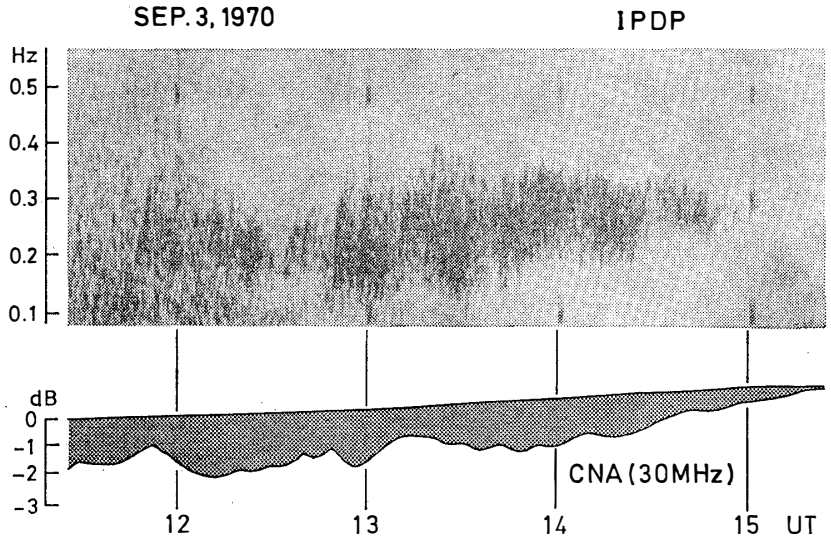

Fig. 47. Example of IPDP events accompanied by intense cosmic noise absorption.

However, proton auroras appear fairly steadily from the evening to the morning, whereas the occurrences of the IPDP events are concentrated in the early evening hours (Fig. 46). Furthermore, large cosmic noise absorption is observed during the IPDP events (Figs. 44 and 47), but proton auroras are seldam accompanied by cosmic noise absorption when the IPDP events are not observed. These facts indicate that IPDP events are generated by high energy ring current protons, whereas proton auroras without IPDP events are generated by low energy ring current protons. The concentration of the occurrences of IPDP events in the early evening hours implies that the high energy ring current protons injected near midnight drift westward and first impinge upon the ionosphere in the early evening region, exciting the ion cyclotron waves. That is, the above observational fact suggests a coupling between high energy ring current protons and the bulge of the plasmasphere as indicated by HEACOCK (1971).

During the IPDP events, positive bays develop, suggesting that the high-latitude positive bays in the evening hours are closely related to the proton precipitation into the ionosphere (Figs. 44 and 45).

6. Summary of Proton Aurora and Electron Aurora Substorms

6.1. Quiet phase

Features of proton auroras and electron auroras during quiet times without a magnetospheric substorm are first summarized.

1) A diffuse proton aurora is present and stationary from the evening to the morning with a fairly constant luminosity (H_β emission of 10–30 R). The zone of proton aurora emission is situated near tne poleward horizon of Syowa Station ($L=10$) in the evening hours, and it gradually moves equatorward before midnight, almost reaching the zenith ($L=6.4$) at midnight. After midnight, the emission zone gradually returns poleward. This emission zone of the diffuse proton aurora is called as 'proton aurora belt'.

2) If the day before a quiet day is disturbed, the luminosity of proton auroras in the evening region increases considerably, though the proton aurora belt is still situated at the same location.

3) In the evening to midnight region, electron auroras are absent in the proton aurora belt. The electron aurora oval is thought to be located on the poleside of the proton aurora belt.

4) After midnight, proton auroras are accompanied by diffuse electron auroras (diffuse glows and patches), *i. e.*, the proton aurora belt and the electron aurora oval overlap.

6.2. Growth phase of magnetospheric substorm

The growth phase of a magnetospheric substorm is defined by a gradual increase in the magnetic field intensity in the distant tail and a simultaneous decrease at the ATS level, usually after the southward turning of the interplanetary magnetic field (Fairfield and Ness, 1970; Aubry and McPherron, 1971; Russell *et al.*, 1971; Meng *et al.*, 1971; Iijima, 1972). On the earth's surface, the growth phase is characterized by an enhancement of the bimodal DP-field in the polar region (Iijima *et al.*, 1968; Iijima and Nagata, 1970, 1971; Kokubun, 1971; Mishin and Grafe, 1971).

The dynamic behavior of proton auroras and electron auroras during the growth phase is summarized in the space-time diagrams in the Fig. 48. From

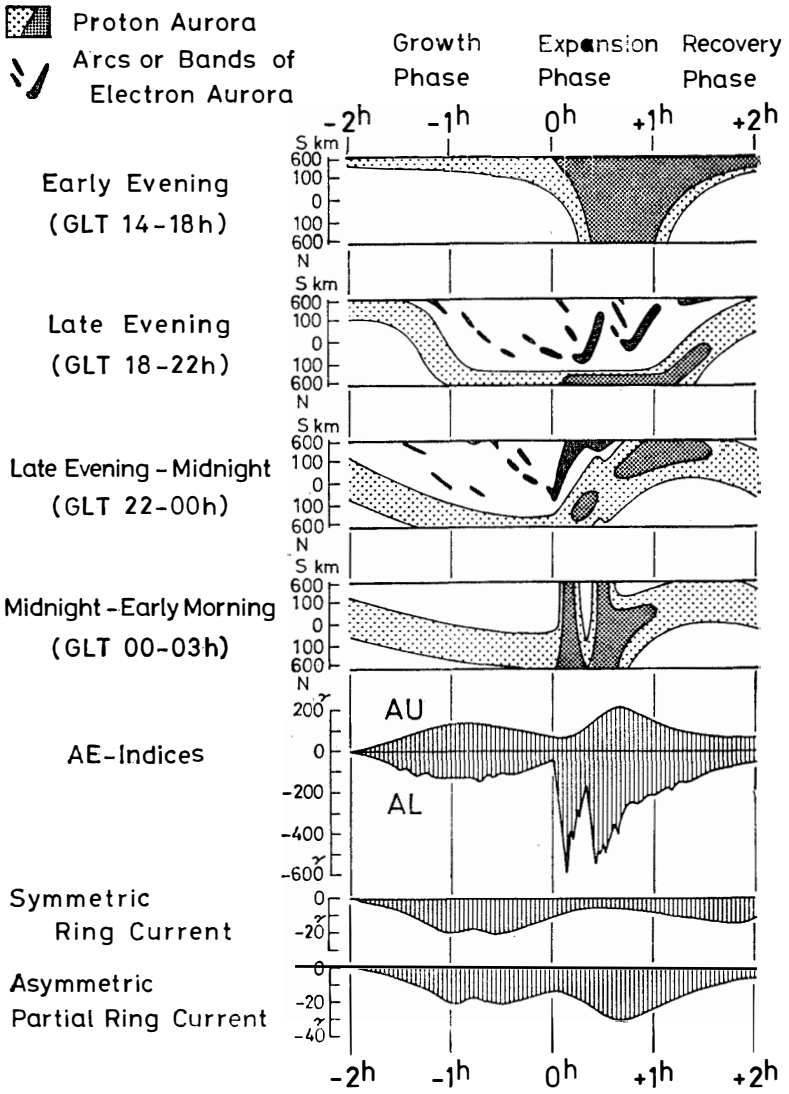

Fig. 48. Schematic space-time diagrams showing the dynamic behavior of proton auroras and electron auroras during a magnetospheric substorm. Increase in AU and AL indices and the symmetric and asymmetric partial ring current intensities are also schematically shown. Proton auroras are observed in dotted regions, whereas breakup-type electron auroras (arcs or bands) in shaded regions. Areas of dense dots are the regions of enhanced hydrogen emission. Diffuse-type electron auroras (patches or rays) are not indicated in these diagrams (cf. Fig. 50).

these space-time diagrams, the worldwide development of the proton aurora and electron aurora substorms is schematically illustrated in Fig. 49.

1) The emission zone of proton auroras moves equatorward with a fairly constant luminosity during the course of the growth phase. The speed of the

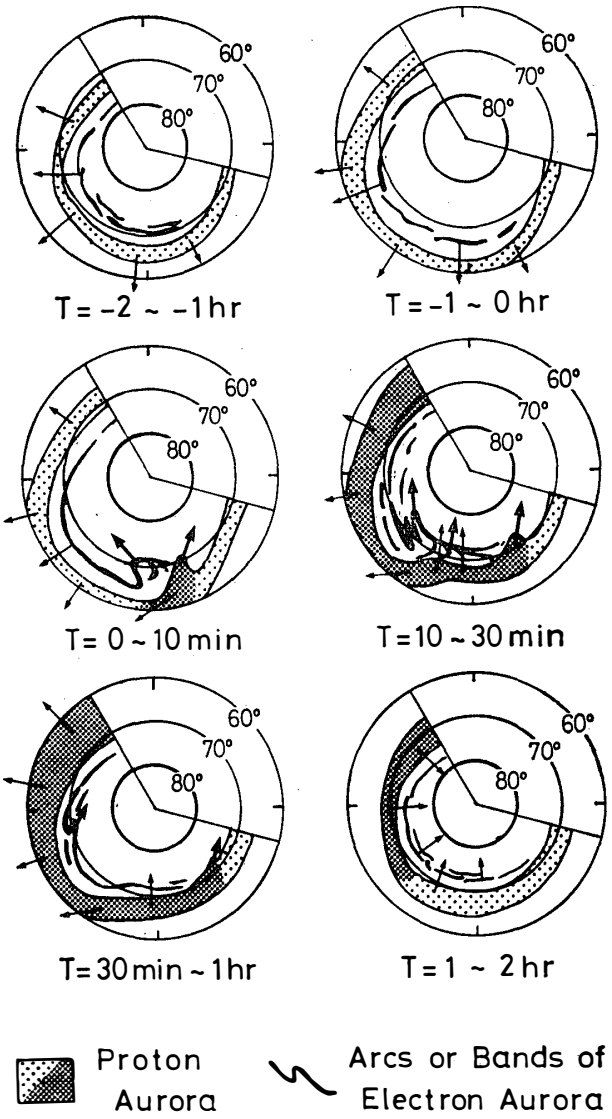

Fig. 49. Schematic diagrams showing the development of proton and electron aurora substorms. T=0 is the onset of the expansion phase. The notation is the same as that in Fig. 48.

equatorward movement strongly depends on the geomagnetic local time with a maximum value of 250 m/sec in the late evening hours (Fig. 27).

2) In the evening to midnight hours, quiet arcs of electron auroras appear on the poleside of the equatorward-shifting proton aurora belt and continue to move equatorward.

3) In association with the equatorward shift of proton aurora belt, the ring current develops. The development of the ring current during the growth phase is characterized by a simultaneous growth of both the symmetric ring current and the asymmetric partial ring current. The center of the partial ring current is located at the late evening region and coincides with the region where the speed of the equatorward shift of the proton auroral emission zone is maximum.

4) The equatorward shift of the emission zone is also related to a positive

deviation in the geomagnetic H component in the evening hours, *i. e.*, the high-latitude positive bay. When the emission zone of proton auroras moves equatorward over the zenith during the positive bay, the deviation of the geomagnetic Z-component from the quiet time values changes from minus to plus (in the southern hemisphere), suggesting the concentration of the eastward current in the emission zone.

6.3. Expansion phase of magnetospheric substorm

The onset of the expansion phase is indicated by a sudden brightening of one of the quiet arcs (electron auroras) near midnight, which is immediately followed by a rapid poleward motion resulting in the auroral bulge (Akasofu substorm $T=0$). The time $T=0$ also corresponds to the time of a sharp increase of AL which denotes the onset of an intense negative bay in the electron aurora bulge (AKASOFU, 1964). The dynamic behavior patterns of proton auroras and electron auroras in the expansion phase are summarized in Figs. 48 and 49. That is;

1) The quiet arcs suddenly brighten in the pre-midnight region at the onset of the expansion phase, and the auroral bulge of electron auroras rapidly expands poleward and westward. Proton auroras are absent in the region of the breakup-type electron auroras.

2) On the other hand, in the post-midnight region, the proton auroras suddenly brighten at the onset of the expansion phase, and the emission zone of proton auroras rapidly expands poleward and probably also eastward. In the region where the proton auroral breakup occurs, breakup-type electron auroras are not observed, but only the weak rayed auroras excited by precipitating electrons appear.

3) The N–S oriented segments appear in the region swept by the leading edge of the expanding electron aurora bulge. Simultaneously with the appearance of the N–S segments, the equatorward-shifted proton aurora belt rapidly recedes poleward with the increase in luminosity (Fig. 33).

4) After the passing of the breakup-type proton auroras in the post-midnight region, the proton aurora belt recedes poleward, and diffuse patches or rays of electron auroras appear equatorward of the proton aurora belt or superimposed on the proton aurora. These diffuse-type electron auroras move eastward and equatoward.

5) In the evening region, the westward traveling surge travels on the poleside of the proton aurora belt along the pre-existing electron auroral arcs without a large poleward expansion of electron aurora bulge. The first appearance of the traveling surge in the late evening region (GLT 18–22h) is approximately 10–30 min after the onset of the expansion phase. The traveling surges are usually observed several times during the expansion phase. The electron auroral arcs move equatorward before the passing of each traveling surge and return poleward after the passing, whereas the equatorward-shifted emission zone of proton auroras does not return poleward during the expansion phase.

6) The emission zone of proton auroras in the evening region expands equatorward with a large increase in luminosity after the onset of the expansion phase. The latitudinal width of the expanding proton aurora belt becomes wider in the earlier local time region, suggesting the earthward diffusion of the westward-drifting ring current protons.

7) In association with the equatorward expansion of the proton aurora belt, an asymmetric partial ring current develops. The center of the partial ring current is situated in the region where the equatorward expansion of the proton aurora belt with a luminosity enhancement is maximum, and it moves from the late evening to the early evening region during the course of the expansion phase.

8) The equatorward expansion of the proton aurora belt is also related to a high-latitude positive H bay in the evening hours. When the emission zone of proton auroras moves equatorward over the zenith, the deviation of the Z component from the quiet time values changes from minus to plus (in the southern hemisphere), suggesting again the eastward concentrated current in the hydrogen emission zone.

9) The occurrences of ULF emissions (IPDP) in the early evening hours after the onset of the expansion phase are simultaneously accompanied by the appearance of proton auroras and cosmic noise absorption.

6.4. Recovery phase of magnetospheric substorm

The beginning of the recovery phase is defined by a decay of both the westward electrojet and the enhanced bimodal DP current. The behaviors of proton auroras and electron auroras in the recovery phase are summarized as follows (cf. Figs. 48 and 49):

1) The poleward and westward expansion of the electron aurora bulge stops in the evening to midnight region.

2) The equatorward-shifted and expanded emission zone of proton auroras in the evening region contracts poleward.

3) Near midnight the poleward recovery of the equatorward-shifted proton aurora belt occurs during the expansion phase. In the recovery phase, the diffuse patches and rays of electron auroras appear superimposed on the poleward-recovered proton aurora belt or equatorward of it in the midnight to morning region.

7. Discussions

7.1. Proton and electron precipitation patterns and the source regions in the magnetosphere

In the studies of the source regions of proton auroras and electron auroras in the magnetosphere, auroras have been classified into two types. One is the breakup-type aurora which is characterized by a rapid poleward motion with a sudden brightening, and the other is the diffuse-type aurora which is characterized by a gradual equatorward movement and a less variation in luminosity. In electron excited auroras, the breakup-type auroras are usually seen as arcs or bands, while the diffuse-type auroras are usually seen as diffuse glow, patches and rays. In proton auroras, the diffuse type auroras are observed as the E–W oriented broad diffuse band, but the forms of the breakup-type proton auroras are unknown, because proton auroras of this type usually appear superimposed on the diffuse type electron auroras in the post-midnight region, and the luminosity is

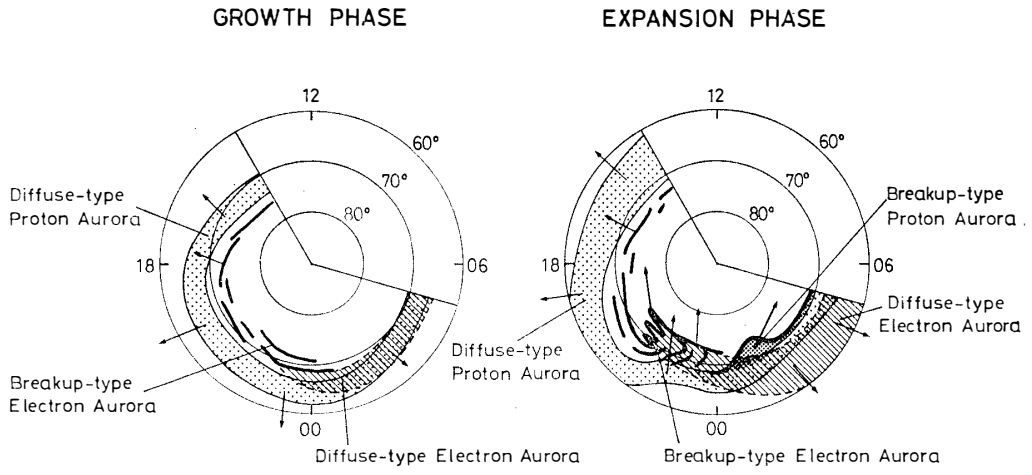

Fig. 50. Schematic diagrams showing the relationship of the locations between breakup-type and diffuse-type auroras.

lower than the luminosity of the diffuse-type electron auroras (Section 4. 3.).

The relationship between the locations of these breakup-type and diffuse-type auroras is schematically illustrated in Fig. 50. In the evening to midnight region, the breakup-type electron auroras (arcs or bands) appear on the poleside of the diffuse-type proton aurora, whereas the breakup-type proton auroras are located on the poleside of the diffuse-type electron auroras in the midnight to morning region. These auroral precipitation patterns in the evening to midnight region coincide with the earlier results of several workers, *i. e.*, proton auroras are located equatorward of electron auroras before midnight (YEVLASHIN, 1963; EATHER and SANDFORD, 1966; WIENS and VALLANCE JONES, 1969; REES and BENEDICT, 1970; MONTBRIAND, 1971). For the midnight to morning region, however, STROFFREGEN and DERBLOM (1962), DERBLOM (1968), and WIENS and VALLANCE JONES (1969) advocated the crossover of the precipitation regions of proton auroras and electron auroras, while EATHER and SANDFORD (1966), REES and BENEDICT (1970), and EATHER and MENDE (1971) showed there was an overlap of both the emission zones. This disagreement is thought to result from the fact that the former workers did not distinguish between the breakup-type proton auroras and the diffuse-type proton auroras due to the low time-resolution of their instruments for proton aurora observation. In the quiet times or during the growth phase of a magnetospheric substorm, diffuse-type proton auroras remain stable with a fairly constant luminosity from the evening to the morning region, and breakup-type proton auroras are absent (Section 3. 2.). That is, diffuse-type proton auroras are superimposed on diffuse-type electron auroras after midnight, and an overlap of both emission zones is observed. However, during the expansion phase of a substorm, breakup-type proton auroras expand poleward with a large enhancement of luminosity, while the diffuse-type electron auroras move equatorward (Section 4. 3.). That is, a cross-over is observed after midnight, with the breakup-type proton aurora located poleward of the diffuse-type electron aurora.

The auroral precipitation patterns shown in Fig. 50 agree well with the results of the local-time survey of the low-energy proton and electron intensities with a low-altitude polar-orbiting satellite Injun 5 by FRANK and ACKERSON (1971 b). They showed that in the evening to midnight region, inverted 'V' electron precipitation bands are present poleward of the diffuse proton precipitation zone, whereas in the midnight to morning region, well-defined bands of relatively high proton intensities are located poleward of the diffuse electron precipitation zone, and these diffuse proton and electron precipitation zones are separated from the inverted 'V' electron precipitation bands and the well-defined proton precipitation bands by the trapping boundary for more energetic electron intensities, $E>45$ kev. The diffuse proton and electron precipitation zones which are located equatorward of the trapping boundary seem to correspond to the emission zones of diffuse-type proton auroras and electron auroras. On the other hand, the inverted 'V' electron precipitation bands which appear poleward of the trapping boundary in the evening to midnight region will correspond to the breakup-type

electron auroras (arcs or bands) as indicated by ACKERSON and FRANK (1972). The well-defined proton precipitation bands observed on the poleside of the trapping boundary in the midnight to morning region are supposed to correspond to the breakup-type proton auroras.

FRANK and ACKERSON (1971 b) interpreted these diffuse electron and proton precipitation zones as the signature to the injection of plasma sheet electrons and protons into the trapping region near midnight and their subsequent eastward and westward drifts accompanied by energization and dissipation into the atmosphere. EATHER and CAROVILLANO (1971) also suggested that the source of the diffuse-type proton auroras is the trapped ring current protons because the ring current protons in the magnetosphere observed by FRANK (1967 b) occupy the interval in L corresponding to the latitudinal extent of the proton aurora. The good correlation between the growth in proton aurora intensities and the development of the asymmetric partial ring current (Section 5. 1.) confirms the suggestion that they are the source of the diffuse-type proton aurora.

As a source region of the inverted 'V' electron precipitation bands located poleward of the trapping boundary, FRANK and ACKERSON (1971 a) proposed the plasma sheet because the energy spectra of electrons in the inverted 'V' precipitation bands are similar to those in the plasma sheet near the magnetic equator observed by FRANK (1967 a). The same idea was also suggested by CHASE (1969) and HONES *et al.* (1971 a). On the other hand, ACKERSON and FRANK (1972) indicated that the source region of the inverted 'V' electron precipitation bands is the magnetosheath.

In the intense breakup-type electron auroras (bright arcs), the spectrum of precipitating electrons shows the near-monoenergetic nature with a pronounced peak in the kev range (ALBERT, 1967; EVANS, 1968; WESTERLUND, 1969). Moreover, the pitch-angle distribution of these precipitating electrons is highly peaked along the geomagnetic field lines (HOFFMAN and EVANS, 1968; VONDRACK *et al.*, 1971; WHALEN and MCDIARMID, 1972; ACKERSON and FRANK, 1972). These facts are interpreted as the signature of the acceleration of plasma-sheet or magnetosheath electrons into the earth's atmosphere due to the upward electric field along the geomagnetic field lines.

As to the spectrum of the precipitating protons which seem to excite the breakup-type proton aurora, RÈME and BOSQUED (1971) observed a similar highly anisotropic pitch-angle distribution peaked near 0° (Fig. 51). They found that the intense proton fluxes with a pronounced anisotropic pitch-angle distribution along the geomagnetic field lines were accompanied by the increase of high-energy electron fluxes of 5–30 kev and the decrease of low-energy electron fluxes of 0. 5 –5 kev. RÈME and BOSQUED (1971) explained this result in terms of the downward electric field parallel to the geomagnetic field lines. That is, a potential difference along the geomagnetic field lines accelerates protons into the atmosphere with a subsequent anisotropic pitch-angle distribution, but this potential barrier repels or slows down precipitating electrons (Fig. 52).

Summarizing the above discussion, it is supposed that the breakup-type pro-

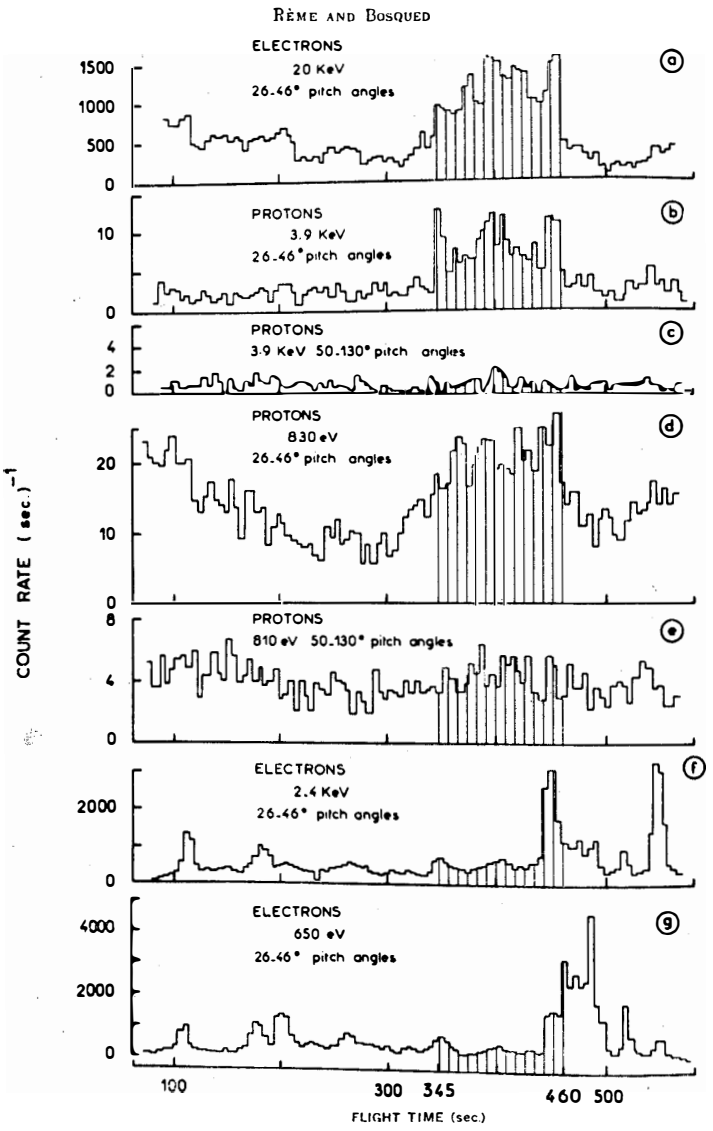

Fig. 51. The 5-sec averaged count rate of various detectors during a rocket flight. A large increase in the precipitating proton flux during the flight time of 345 to 460 sec was accompanied by the enhanced flux of high energy electrons, but the flux of low energy electrons scarcely increased (after RÈME and BOSQUED, 1971).

ton and electron auroras are excited by plasma-sheet or magnetosheath protons and electrons which are accelerated towards the atmosphere due to the downward and upward electric fields parallel to the geomagnetic field lines. The breakup-

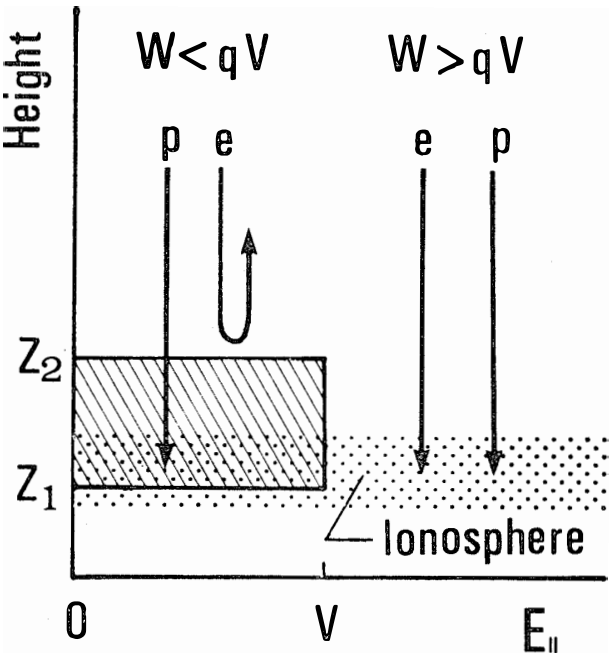

Fig. 52. Effect of the potential difference along the geomagnetic field lines on precipitating electrons and protons. Assuming that a potential difference V is present in the height interval from Z_1 to Z_2 and q is the particle charge, electrons with energy less than qV are repelled by this potential barrier, but protons are accelerated and gain the energy of qV.

type electron auroras and proton auroras appear in the pre-midnight and post-midnight regions, respectively. Moreover, proton auroras are absent in the emission region of breakup-type electron auroras, while breakup-type electron auroras are absent in the emission region of breakup-type proton auroras (Sections 4. 2., 4. 3.). These facts suggest that the direction of the parallel electric field is upward in the pre-midnight region so as to accelerate electrons into the atmosphere,

Table 4. Relationship between the auroral precipitation patterns and their source regions in the magnetosphere.

	Type of aurora	Longitudinal location	Latitudinal location	Source in the magnetosphere
Electron aurora	Breakup-type (Arc and band)	Evening-midnight	Poleside of the trapping boundary	Plasma sheet electrons
	Diffuse-type (Diffuse glow, patch and ray)	Midnight-morning	Equatorside of the trapping boundary	Trapped electrons
Proton aurora	Breakup-type	Midnight-morning	Poleside of the trapping boundary	Plasma sheet protons
	Diffuse-type (Diffuse band)	Evening-morning	Equatorside of the trapping boundary	Ring current protons

whereas the electric field is downward in the post-midnight region and results in the acceleration of protons. A generation mechanism of the breakup-type proton auroras and electron auroras is further discussed in Section 7. 3. The relationship between the auroral precipitation patterns and their source regions in the magnetosphere is summarized in Table 4.

7.2. Equatorward movement of the proton auroral precipitation belt during the growth phase of a magnetospheric substorm and its relationship with the magnetospheric convection

The diffuse-type proton aurora (proton aurora belt) and the breakup-type electron aurora (quiet arcs) lying poleward of it continue to move equatorward during the growth phase of a magnetospheric substorm (Section 4.1.). Sources of the diffuse-type proton aurora and the breakup-type electron aurora have been suggested to be the ring current protons and plasma sheet electrons in Section 7.1. Therefore, equatorward shifts of the diffuse-type proton aurora and the breakup-type electron aurora indicate earthward movement of the ring current and the plasma sheet. Since the trapping boundary for energetic electrons, $E>45$ kev is thought to be present between the diffuse-type proton aurora and the breakup-type electron aurora, these equatorward motions also indicate the contraction of the closed field-line region and the expansion of the polar cap region whose field lines extend into the tail. This feature will reflect the change in the tail field configuration due to the flux transport from the dayside magnetopause to the tail, suggested by AUBRY *et al.* (1970), FAIRFIELD and NESS (1970), AUBRY and MCPHERRON (1971), MENG *et al.* (1971) and MCPHERRON *et al.* (1972). The luminosity of breakup-type electron auroras fluctuates rapidly during the growth phase, whereas diffuse-type proton auroras are present with fairly constant intensities. Therefore, the diffuse-type proton aurora is useful as a probe of the magnetospheric convection.

The speed of the equatorward movement of the proton aurora belt during the growth phase is 100–250 m/sec with a maximum value in the late evening region. The corresponding speed of the earthward motion on the equatorial plane in the magnetosphere is 4–10 km/sec at $L\sim6$, and the magnitude of the dawn-dusk electric field driving the earthward movement is approximately 0. 5–1. 2 mV/m. This drifting speed of the magnetospheric plasma and the magnitude of the corresponding dawn-dusk electric field is comparable to the values estimated by previous workers, *i. e.*, 12 km/sec and 0. 24 mV/m at $L=6-10$ (VASYLIUNAS, 1968), 5. 5 km/sec and 0. 6 mV/m at $L=6-9.7$ (SCHIELD and FRANK, 1970), and 3 km/sec and 0. 36 mV/m at $L=6.6$ (SHELLEY *et al.*, 1971). The large earthward displacement of the ring current protons results in the intensification of the ring current due to the betatron and Fermi acceleration processes (AXFORD, 1969; WOLF, 1970; SWIFT, 1971). If the equatorward movement of aurora with a speed of 250 m/sec, which is a typical value in the late evening hours, lasts for 1 hour during the growth phase, the total displacement of the proton aurora belt is approximately 8° in latitude. By mapping on to the equatorial plane through the FAIRFIELD

(1968) model of the magnetic field, this equatorward movement corresponds to the earthward approach of the ring current protons from $L=10$ to $L=5$, resulting in the energization of protons. The original energy of the ring current protons increases approximately sevenfold as they are shifted inward. The energization of the ring current protons through the earthward movement explains a close correlation between the growth of the ring current and the equatorward movement of the proton aurora belt (Figs. 41 and 42). In particular the asymmetric growth of the ring current during the growth phase can be explained by this mechanism because the center of the growing asymmetric partial ring current is in the region where the speed of the equatorward movement is maximum.

During the growth phase of a substorm, the equatorward movement of the proton aurora belt and the development of the asymmetric partial ring current in the evening region are accompanied by the growth of a positive H bay. When the proton aurora belt moves equatorward over the zenith, the deviation of the geomagnetic Z-component from the quiet time values changes from minus to plus (in the southern hemisphere), suggesting the concentration of eastward current in the emission region of proton auroras (Section 5. 1.). Since the westward electrojet scarcely shows any development during the growth phase, the concentrated eastward current cannot be explained by a return current of the westward electrojet. Other interpretation for this concentrated eastward current in the evening region during the growth phase are as follows (IIJIMA and NAGATA, 1971).

1) An enhancement of eastward auroral-zone current in the bimodal DP current (DP 2) due to the increase in the ionospheric conductivity under the condition of the intensified dawn-dusk electric field in the magnetosphere (IIJIMA and NAGATA, 1970).

2) The appearance of additional concentrated eastward current, which is fed by the partial westward ring current in the dusk region of the magnetosphere through the field aligned currents due to the increase in the ionospheric conductivity (CUMMINGS *et al.*, 1968; KAMIDE and FUKUSHIMA, 1972).

It is not yet known which interpretaion is better for the concentrated eastward current during the growth phase. However, both mechanisms require an increase in the ionospheric conductivity. The location of the concentrated eastward current coincides with the location of the proton aurora belt, and in this region electron auroras are absent. Therefore, it is concluded that the increase in the ionospheric conductivity results from the proton precipitation. Using the ionization rates calculated by EATHER and BURROWS (1966) and corrected by EATHER (1967 b), the ionospheric conductivity can be estimated. If the initial energy spectrum is represented by a power-law function of E^{-2} and the total flux between 1 kev and 1,000 kev is assumed to be $10^7/cm^2$ sec ster, which is required to excite about 50 R of H_β emission, the maximum density of the secondary electrons is $6.0\times10^4/cm^3$ at 105 km and the integrated electron density per unit cross-section in the dynamo region between 90 and 120 km is $1.4\times10^{11}/cm^2$. The subsequent height-integrated Hall and Cowling conductivities are approximately 5 and 15 mho, respectively. Assuming that the width of the proton

precipitation zone is 5° and the intensity of the electric field is 10 mV/m, the total Cowling current is 7.8×10^4 amperes. On the ground beneath this eastward Cowling current, the induced positive variation of the geomagnetic H component is about 160γ. The estimated value of the positive H variation seems to be sufficient for the explanation of the observed positive bays in the evening hours.

7.3. Generation mechanism of the proton and electron aurora beakup

At the onset of the expansion phase of a magnetospheric substorm, the breakup-type electron aurora (quiet arcs) lying on the pole-side of the trapping boundary in the pre-midnight region rapidly expands poleward and westward with a sudden brightening, whereas the breakup-type proton aurora located on the pole-side of the trapping boundary in the post-midnight region expands poleward and eastward (Section 6. 3.). In Section 7.1., it is indicated that the breakup-type proton and electron auroras are thought to be excited by plasma sheet protons and electrons which are accelerated towards the atmosphere due to the downward and upward electric fields along the geomagnetic field lines, respectively. This electrostatic acceleration can be explained by the growth of an anomalous resistivity along the magnetic field lines (FÄLTHAMMAR, 1969; AKASOFU, 1969; RÈME and BOSQUED, 1971). Mechanisms of an anomalous resistivity were given by SWIFT (1965), OSSAKOW (1968), and KINDEL and KENNEL (1971). SWIFT (1965) and OSSAKOW (1968) attributed an anomalous resistivity to an unstable growth of the ion acoustic wave by field-aligned currents. KINDEL and KENNEL (1971) showed that the electrostatic ion cyclotron wave is more unstable under small field-aligned currents than the ion acoustic wave, for a wide range of Te/Ti.

If the dawn-dusk electric field in the magnetosphere is intensified during the course of the growth phase, Pedersen and Hall currents in the ionosphere become strong due to the coupling between the magnetosphere and the ionosphere through the high conductivity along the field lines. This ionospheric current is connected with the magnetospheric current through the field-aligned current, because the ionospheric current has a nonzero divergence (the growth of the Hall current in the ionoshere is observed as a development of the bimodal DP field, Section 4.1.). The direction of the field-aligned current is from the magnetosphere to the ionosphere in the midnight to morning region, and opposite in the evening to midnight region. When the increasing field-aligned current exceeds a critical value, field-aligned anomalous resistivity grows due to the current-driven instability. The generated potential drop along the geomagnetic field lines accelerates protons and electrons towards the atmosphere in the morning and evening regions, respectively (Fig. 53). The ionospheric conductivities increase by the precipitation of these accelerated protons and electrons, and the westward electrojet grows rapidly. The growth of the westward electrojet results in the intensification of the field-aligned current through the continuity of the current, contributing to the increase of the current-driven anomalous resistivity. As a result, the electrons and protons accelerate towards the atmosphere even more vigorously. That is, a positive feedback loop for the auroral breakup is constructed. This feedback

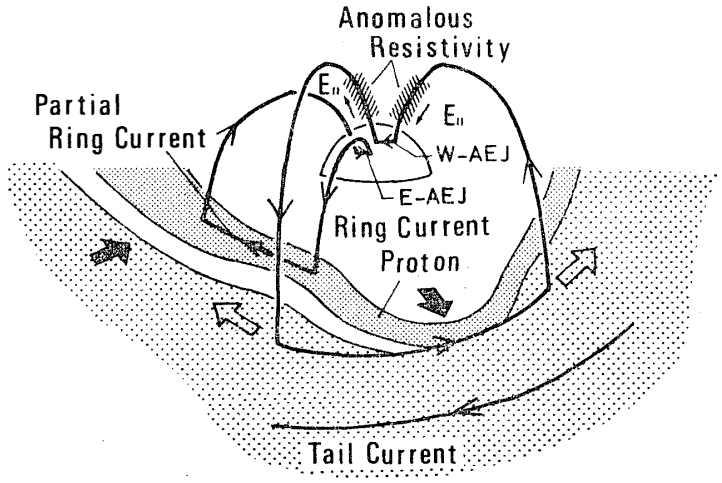

Fig. 53. Schematic diagram showing the breakup mechanism of the proton aurora in the post-midnight region and the electron aurora in the pre-midnight region, and the subsequent development of the partial ring current due to the proton injection.

system will continue to grow until the field-aligned conductivity becomes as low as the ionospheric conductivity in the electrojet. The magnitude of the Pedersen conductivity and the current density in the electrojet are approximately 10^{-4}mho/m and 10^{-6}amp/m^2. Assuming that the height of the anomalous resistivity region is 1000 km, the maximum value of the generated potential difference along the field lines is approximately 10 kV. This magnitude is consistent with the values of 1–2 kV and 7 kV which were estimated from the anisotropic pitch-angle distributions of the precipitating protons and electrons by RÈME and BOSQUED (1971) and WHALEN and MCDIARMID (1972), respectively.

A similar positive feedback mechanism for the auroral breakup event was presented by OGUTI (1971). CORONITI and KENNEL (1972) also explained the equatorward polarization of the electric field in the ionosphere at the onset of the expansion phase by the growth of the current-driven anomalous resistivity in the north-south current sheet along the auroral oval.

7.4. Dynamic behavior of the injected ring current protons and associated phenomena during the expansion phase of a magnetospheric substorm

The precipitation of the plasma sheet protons and electrons results in the disappearance of the near-earth tail current. This feature is observed as a geomagnetic collapse near midnight (LEZNIAK and WINCKLER, 1970; MCPHERRON *et al.*, 1972). As the proton breakup event in the midnight to morning region causes the dissipation of plasma sheet protons into the atmosphere, it is reasonable that the disappearance of the ring current in this local-time region is observed after the onset of the expansion phase as indicated by AKASOFU (1968).

The N–S oriented segments (MONTBRIAND, 1971) appear in the region swept

by the leading edge of the expanding electron aurora bulge in the late evening to midnight region. Simultaneously with the appearance of the N–S segments, the equatorward-shifted proton aurora belt rapidly returns poleward with the increase in luminosity (Section 4. 2.). The rapid poleward recovery of the proton aurora belt is interpreted as the tailward drift of the trapped ring current protons due to the electric field induced by the geomagnetic collapse. The subsequent eastward polarization current near the edge of the plasma sheet is capable of feeding the westward electrojet by the coupling to the ionosphere through the field-aligned current (Fig. 53).

In contrast to the rapid poleward recovery of the equatorward-shifted proton aurora belt near midnight after the passing of the traveling surge of the electron aurora, the proton aurora belt continues to move equatorward expanding in width in the evening region during the expansion phase. The spreading of latitudinal width of the proton aurora belt is better seen in the earlier local-time region, suggesting a radial diffusion of the westward-drifting protons. The poleward recovery of the proton aurora belt begins in the recovery phase. Therefore, the intensified dawn-dusk electric field is thought to be present during the expansion phase in the magnetosphere.

The increase in luminosity of proton aurora after the onset of the expansion phase is thought to result from the injection of the protons accelerated by the collapse of the geomagnetic tail. The injection of plasma sheet protons and electrons into the trapping region near midnight has been observed by many workers (ARNOLDY and CHAN, 1969; PFITZER and WINCKLER, 1969; LEZNIAK and WINKLER, 1970; FRANK, 1970; AARSNES *et al.*, 1970; DEFOREST and MCILWAIN, 1971). Injected protons and electrons drift westward and eastward during their precipitation into the atmosphere due to a pitch-angle diffusion. These precipitating protons and electrons will excite the diffuse-type proton aurora in the evening region and the diffuse-type electron aurora in the morning region.

Simultaneously with a large increase in luminosity of proton auroras and a spreading of the width of the proton aurora belt in the evening region, the asymmetric partial ring current develops. The center of the partial ring current moves westward from the late evening to the afternoon region during the course of the expansion phase (PUDOVKIN *et al.*, 1968; KAMIDE and FUKUSHIMA, 1972; and in Section 5.1. of this paper). This feature is different from the behavior of the asymmetric partial ring current during the growth phase, *i. e.*, in the growth phase, the center moves eastward from the early evening to the late evening region, or remains in the late evening region (Fig. 42). These results confirm that the source of both the diffuse-type proton aurora and the asymmetric partial ring current is the westward and also earthward drifting protons injected near midnight after the onset of the expansion phase.

As to the loss mechanism of the ring current protons, CORNWALL *et al.* (1970, 1971) put forward the idea of an ion cyclotron turbulent precipitation due to the coupling between the ring current protons and the plasmasphere, *i. e.*, ring current protons, which are unaffected by ion cyclotron waves outside the plasma-

sphere, undergo strong turbulent diffusion just inside the plasmapause. EATHER and CAROVILLANO (1971) on the other hand calculated the lifetime of the ring current protons by using a theory by GENDRIN (1968) concerning the interaction between low energy protons and ion cyclotron waves. They found that a pitch-angle diffusion is more efficient at higher L shells and for lower energy ring current protons, *i. e.*, the ring current protons with lower energies precipitate more quickly at higher L shells outside the plasmasphere (Fig. 54).

In Section 5. 2., it is indicated that the occurrence of the geomagnetic micropulsation IPDP event, which is thought to be generated by the ion cyclotron instability (HEACOCK, 1967; FUKUNISHI, 1969; SAITO, 1969; GULYEL'MI *et al.*, 1970; GENDRIN, 1970), is accompanied by the appearance of proton aurora and a large enhancement of cosmic noise absorption. (HEACOCK (1968) also observed a close correlation between IPDP event and cosmic noise absorption.) This relationship can be interpreted as a signature of proton precipitation into the atmosphere caused by ion cyclotron waves (IPDP event). However, the close relationship between proton auroras and IPDP events is not observed in all local-time regions. Proton auroras appear from the evening to the morning, whereas the occurrences of IPDP events are concentrated in the early evening region (Fig.

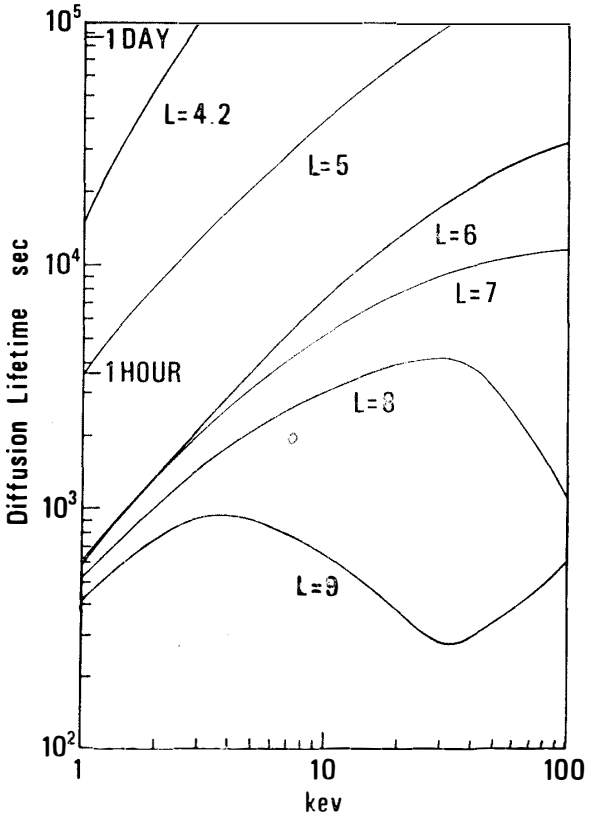

Fig. 54. Diffusion lifetime of trapped protons as a function of energy (after EATHER and CAROVILLANO, 1971).

46). Moreover, proton auroras are not accompanied by a distinct increase in cosmic noise absorption when IPDP events are absent. Using the calculation result of EATHER and BURROWS (1966) corrected by EATHER (1967 b), the absorption of cosmic radio noise due to the proton precipitation can be estimated. If the initial energy spectrum is represented by a power-law function of E^{-2}, with $1\,\text{kev} \leq E \leq 1$ Mev and the total flux is assumed to be $10^7/\text{cm}^2$ sec ster, which is required to excite about 50 R of H_β emission, the corresponding CNA increase is only 0.05 dB at 27.6 MHz. Therefore, it is natural that proton auroras are not usually accompanied by the enhancement of cosmic noise absorption. However, a large increase in CNA (0.1–1 dB at 30 MHz) during the IPDP event must be explained by an increase in the electron density in the ionosphere due to the ionization of precipitating protons, because of the absence of electron auroras. This suggests that the energy of protons generating IPDP events is fairly high. Assuming that the initial energy spectrum is E^{-1}, with $1\,\text{kev} \leq E \leq 1$ Mev and the total flux is $10^6/\text{cm}^2$ sec ster, the increase in cosmic noise absorption is about 0.2 dB at 27.6 MHz and the intensity of the excited H_β emission is approximately 30 R. Unfortunately, from the observation of Doppler shift in H_β emissions, little information on the energy spectrum of precipitating protons during IPDP events can be obtained, because the Doppler shift in hydrogen emission lines is almost unchanged when the initial energy of protons exceeds 100 kev (CHAMBERLAIN, 1961).

The concentration of IPDP occurrences in the early evening region can be interpreted as a coupling between the plasmasphere bulge and the westward-drifting protons as suggested by HEACOCK (1971). CHAPPELL *et al.* (1971) showed that the night-side plasmasphere is convected to lower L shells, whereas the outermost edge of the dayside plasmasphere and the bulge region are peeled off and convected sunward, following an enhanced convection during the magnetospheric substorm. Therefore, as a loss mechanism of high energy ($\gtrsim 50$ kev) protons injected near midnight after the onset of the expansion phase, it will be possible that the injected protons drift westward and enter the sunward-convecting bulge in the early evening sector, resulting in the generation of intense ion cyclotron waves (IPDP events) and their dissipation into the atmosphere. Precipitating high energy protons will excite proton auroras and cause cosmic noise absorption. On the other hand, low energy (< 50 kev) protons injected near midnight are thought to drift westward gradually, precipitating into the atmosphere due to a pitch-angle diffusion mechanism proposed by EATHER and CAROVILLANO (1971) or other unknown loss mechanisms.

In the evening region, the rapid equatorward expansion of the proton aurora belt with a large increase in luminosity during the expansion phase is accompanied by the development of a positive H bay. When the proton aurora belt moves equatorward over the zenith, the deviation of the geomagnetic Z component from the quiet time values changes from minus to plus (in the southern hemisphere), suggesting the concentration of eastward current in the proton atrora belt (Section 5.1.). This close correlation between asymmetric partial ring current,

positive bay and proton aurora during the expansion phase indicates that a positive bay results from the additional concentrated eastward current which is fed by the partial ring current through the field-aligned current due to the increase in the ionospheric conductivity in the proton aurora belt (CUMMINGS *et al.*, 1968; KAMIDE and FUKUSHIMA, 1972). In Section 7.2., it has already been indicated that the proton flux required to excite the observed H_β emission is sufficient for the increase in the ionospheric conductivity.

In contrast to the phenomena associated with the injection of protons in the evening region, the events associated with the electron injection are observed in the morning region, *i. e.*, diffuse-type electron auroras instead of diffuse-type proton auroras, gradual negative bays instead of gradual positive bays, and VLF emissions in place of ULF emissions and so on. However, these phenomena associated with electron injection will not be discussed in this paper (cf. HIRASAWA and NAGATA, 1972).

8. Conclusions

Concerning the constitution of proton aurora and electron aurora substorms and the generation mechanism of a magnetospheric substorm, the following conclusions are obtained.

8.1. Quiet phase

1) The emission zone of diffuse-type proton auroras (proton aurora belt) is present with a fairly constant luminosity from the evening to the morning. The source of the diffuse-type proton aurora is thought to be quiet-time ring current protons.

2) The location of the proton aurora belt is situated equatorward of the breakup-type electron auroras in the evening to midnight region, and it is superimposed on the emission zone of the diffuse-type electron auroras after midnight.

8.2. Growth phase

1) The proton aurora belt and the quiet arcs lying poleward of it continue to move equatorward during the growth phase. The speed of the equatorward movement of the proton aurora belt strongly depends on the geomagnetic local time with a maximum value of 250 m/sec in the late evening region. This auroral movement will reflect the earthward movement of the ring current protons due to the intensification of the magnetospheric convection.

2) The equatorward movement of the proton aurora belt is accompanied by the growth of an asymmetric ring current, which has its maximum intensity in the late evening region. The asymmetric development of the ring current can be explained by the most effective energization of ring current protons in this region through the betatron and Fermi acceleration processes during their earthward movement, because the speed of the equatorward movement of the proton aurora belt is fastest in the evening hours, which suggests that the earthward displacement of the ring current protons is maximum in this local-time region.

3) When the proton aurora belt moves equatorward over the zenith of Syowa Station accompanying the development of the positive H bay, the deviation of the geomagnetic Z component from the quiet time values changes from minus to

plus (in the southern hemisphere), suggesting the concentration of the eastward current in the proton aurora belt. It is indicated that the increase in the ionospheric conductivity due to the precipitating protons required to excite the observed proton aurora luminosity is sufficient for the concentration of the eastward current.

8.3. Expansion phase

1) The quiet arcs suddenly brighten in the pre-midnight region, and the electron aurora bulge rapidly expands poleward and westward. Proton auroras are absent in the leading edge of the expanding bulge, whereas in the post-midnight region, the proton auroras suddenly brighten at the onset of the expansion phase, and the emission zone of the proton auroras rapidly expands poleward and eastward. In the expanding proton aurora bulge, breakup-type electron auroras (arcs or bands) are not observed. It is suggested that there is a mechanism which accelerates protons along the geomanetic field lines from the magnetosphere down to the ionosphere in the post-midnight region and electrons in the pre-midnight region through the current-driven anomalous resistivity, and the auroral breakup event takes place when a positive feedback system is formed, as a result of the growth of field-aligned currents in the above mechanism.

2) In the region swept by the leading edge of the expanding electron aurora bulge, the equatorward-shifted proton aurora belt returns poleward. This rapid poleward recovery is interpreted as the tailward drift of the ring current protons due to the electric field induced by the geomagnetic collapse near midnight.

3) In the evening region, the luminosity of the proton aurora greatly increases and simultaneously the emission zone expands equatorward sometime after the onset of the expansion phase. The latitudinal width of the expanding proton aurora belt becomes wider in the earlier local-time region. These features can be explained by an injection of protons into the trapping region due to the magnetic collapse in the tail, and the subsequent westward and earthward drift.

4) The large increase in the proton aurora luminosity in the evening region is also accompanied by a development of the partial ring current in this local-time region. The center of the partial ring current moves westward from the late evening to the early evening, suggesting the westward drift of the injected ring current protons. Simultaneously with the development of the partial ring current, a positive H bay grows, and the deviation of the geomagnetic Z component from the quiet time values changes from minus to plus when the proton aurora belt shifts equatorward over the zenith of Syowa Station. From this relationship, a positive bay is thought to result from the appearance of the additional concentrated eastward current, which is fed by the partial ring current through the field-aligned currents due to an enhancement of the ionospheric conductivity by the proton precipitation.

5) In the early evening region, the occurrence of an IPDP event is simultaneously accompanied by the appearance of proton aurora and the increase in cosmic noise absorption. This observational fact indicates that the high energy

($\gtrsim$ 50 kev) protons injected near midnight drift westward and enter the sunward-convecting bulge of the plasmasphere at the early evening region, resulting in the generation of intense ion cyclotron waves (IPDP events) and the precipitation of protons into the ionosphere.

6) In the midnight to morning region, diffuse-type electron auroras (diffuse patches or rays) appear equatorward of the proton aurora belt or superimposed on the proton aurora, and they move equatorward and eastward. The source of these diffuse-type electron auroras is thought to be the eastward-drifting electrons injected into the trapping region due to the geomagnetic collapse in the plasma sheet.

8.4. Recovery phase

1) The poleward and westward expansion of the electron aurora bulge stops, and the equatorward-shifted and expanded proton aurora belt in the evening region contracts poleward. This is explained by the decay of the magnetospheric convection and the dissipation of the enhanced ring current protons.

2) In the morning region, diffuse type electron auroras continue to be present superimposed on the proton auroras, or equatorward of the proton aurora belt.

Observation of the proton aurora substorm using the meridian-scanning photometric system with a high time resolution presented much useful information on the generation mechanism of the magnetospheric substorm. Especially, the proton aurora is shown to be utilized as a probe of the magnetospheric convection during the growth phase. It is also suggested that the observation of proton auroras is vital for the study of the breakup mechanism of a substorm. In this respect, simultaneous observations of the rapid dynamic behavior patterns of proton auroras and electron auroras at several stations in the polar region should yield more significant information.

Acknowledgments

The authors wish to express their thanks to all members of the 11th wintering party of the Japanese Antarctic Research Expedition for their kind support in making the observations at Syowa Station, Antarctica. Special thanks are due to Prof. T. OBAYASHI, Drs. A. NISHIDA, T. IIJIMA, T. HIRASAWA and Y. KAMIDE for their valuable discussions. The authors would also like to thank Profs. T. NAGATA, N. FUKUSHIMA and T. OGUTI for their kind encouragement and advice.

Most of the geomagnetic data used in this study are supplied through the World Data Center C 2 for Geomagnetism in Kyoto or the International Geophysical Data Library of the Science Council of Japan. The writers wish to express their thanks to these organizations, and also for individual magnetic observatories all over the world.

The authors are especially grateful to the following institutions for sending the geomagnetic data at the author's request.

a) Geophysical Observatory of New Zealand for the data at Scott Base.
b) Geophysical Branch, Bureau of Mineral Resources, Australia for the data at Mawson and Wilkes.
c) Geophysical Department, Arctic and Antarctic Research Institute of USSR for the data at Novolazarevskaya and Molodezhnaya.
d) World Data Center B-2 for the data at Cape Chelyuskin, Dixon Island, Tixie Bay and Cape Wellen.

References

AARSNES, K., R. AMUNDSEN, H. R. LINDALEN, and F. SØRAAS (1970): Proton precipitation in the noon-midnight meridian and its relation to geomagnetic activity. Physica Norvegica, **4**, 73–83.

ACKERSON, K. L., and L. A. FRANK (1972): Correlated satellite measurements of low-energy electron precipitation and ground-based observations of a visible auroral arc. J. Geophys. Res., **77**, 1128–1136.

AKASOFU, S.-I. (1963): The dynamical morphology of the aurora polaris. J. Geophys. Res., **68**, 1667–1673.

AKASOFU, S.-I. (1964): The development of the auroral substorm. Planet. Space Sci., **12**, 273–282.

AKASOFU, S.-I. (1968): Polar and magnetospheric substorms. D. Reidel, Dordrecht, Holland, p. 1–280.

AKASOFU, S.-I. (1969): A model current system for the magnetospheric substorm. Particles and Fields in the Magnetosphere, edited by B. M. MCCORMAC, D. Reidel, Dordrecht, Holland, p. 34–45.

AKASOFU. S.-I., S. CHAPMAN (1964): On the asymmetric development of magnetic storm fields in low and middle latitudes. Planet. Space Sci., **12**, 607–626.

AKASOFU, S.-I., and C.-I. MENG (1969): A study of polar magnetic substorms. J. Geophys. Res., **74**, 293–313.

ALBERT, R. D. (1967): Energy and flux variations of nearly monoenergetic auroral electrons. J. Geophys. Res., **72**, 5811–5815.

ARMSTRONG, J. C., and A. J. ZMUDA (1970): Field-aligned current at 1100 km in the auroral region measured by satellite. J. Geophys. Res., **75**, 7122–7127.

ARNOLDY, R. L., and K. W. CHAN (1964): Particle substorms observed at the geostationary orbit. J. Geophys. Res., **74**, 5019–5028.

ATKINSON, G. (1967): The current system of geomagnetic bays. J. Geophys. Res., **72**, 6063–6067.

AUBRY, M. P., C. T. RUSSELL, and M. G. KIVELSON (1971): On inward motion of the magnetopause before a substorm. J. Geophys. Res., **75**, 7018–7031.

AUBRY, M. P., and R. L. MCPHERRON (1971): Magnetotail changes in relation to the solar wind magnetic field and magnetospheric substorms. J. Geophys. Res., **76**, 4381–4401.

AXFORD, W. I. (1969): Magnetospheric convection. Rev. Geophys., **7**, 421–459.

BOSTROM, R. (1968): Currents in the ionosphere and magnetosphere. Ann. Géophys., **24**, 681–694.

CHAMBERLAIN, J. W. (1961): Physics of the aurora and airglow. Academic Press, New York, p. 1–704.

CHAPPELL, C. R., K. K. HARRIS, and G. W. SHARP (1971): The dayside of the plasmasphere. J. Geophys. Res., **76**, 7632–7647.

CHASE, L. M. (1969): Evidence that the plasma sheet is the source of auroral electrons. J. Geophys. Res., **74**, 348–350.

CLOUTIER, P. A., H. R. ANDERSON, R. J. PARK, R. R. VONDRAK, R. J. SPIGER, and B. R. SANDEL (1970): Detection of geomagnetically aligned currents associated with an auroral arc. J. Geophys. Res., **75**, 2595–2600.

CORNWALL, J. M., F. V. CORONITI, and R. M. THORNE (1970): Turbulent loss of ring current protons. J. Geophys. Res., **75**, 4699–4709.

CORNWALL, J. M., F. V. CORONITI, and R. M. THORNE (1971): Unified theory of SAR arc formation at the plasmapause. J. Geophys. Res., **76**, 4428–4445.

CORONITI, F. V., and C. F. KENNEL (1971): Magnetopause motions, DP-2 and the growth phase of magnetospheric substorms. Preprint of Plasma Physics Group, Univ. Calif., PPG-99.

CORONITI, F. V., and C. F. KENNEL (1972): Polarization of the auroral electrojet. J. Geophys. Res., **77**, 2835–2850.

CUMMINGS, W. D., J. N. BARFIELD, and P. J. COLEMAN (1968): Magnetospheric substorms observed at the synchronous orbit. J. Geophys. Res., **73**, 6687–6698.

DAVIDSON, G. T. (1965): Expected spatial distribution of low-energy protons precipitated in the auroral zones. J. Geophys. Res., **70**, 1061–1068.

DAVIS, T. N. (1962): The morphology of the aurora display of 1957–1958, I. Statistical analysis of Alaska data. J. Geophys. Res., **67**, 59–74.

DAVIS, T. N., and M. SUGIURA (1966): Auroral electrojet activity index AE and its universal time variation. J. Geophys. Res., **71**, 785–801.

DEFOREST, S. E., and C. E. MCILWAIN (1971): Plasma clouds in the magnetosphere. J. Geophys. Res., **76**, 3587–3611.

DERBLOM, H. (1968): On the location of hydrogen emissions with respect auroral forms. Ann. Géophys., **24**, 163–166.

EATHER, R. H. (1967a): Secondary processes in proton auroras. J. Geophys. Res., **72**, 1481–1490.

EATHER, R. H. (1967b): Auroral proton precipitation and hydrogen emissions. Rev. Geophys., **5**, 207–285.

EATHER, R. H., and K. M. BURROWS (1966): Excitation and ionization by auroral protons. Aust. J. Phys., **19**, 309–322.

EATHER, R. H., and R. L. CAROVILLANO (1971): The ring current as the source region for proton auroras. Cosmic Electrodynamics, **2**, 105–132.

EATHER, R. H., and F. JACKA (1966): Auroral hydrogen emission. Aust. J. Phys., **19**, 241–274.

EATHER, R. H., and S. B. MENDE (1971): Airborne observations of auroral precipitation patterns. J. Geophys. Res., **76**, 1746–1755.

EATHER, R. H., and D. L. REASONER (1969): Spectrophotometry of faint light sources with a tilting-filter photometer. Appl. Opt., 8, 227–242.

EATHER, R. H., and B. P. SANDFORD (1966): The zone of hydrogen emission in the night sky. Aust. J. Phys., **19**, 25–33.

EVANS, D. S. (1968): The observations of a near monoenergetic flux of auroral electrons. J. Geophys. Res., **73**, 2315–2323.

FAIRFIELD, D. H. (1968): Average magnetic field configuration of the outer magnetosphere. J. Geophys. Res., **73**, 7329–7338.

FAIRFIELD, D. H., and N. F. NESS (1970): Configuration of the geomagnetic tail during substorms. J. Geophys. Res., **75**, 7032–7047.

FÄLTHAMMAR, C.-G. (1969): Fundamental electromagnetic processes in the outer magnetosphere. Atmospheric Emissions, edited by B. M. MCCORMAC and A. OMHOLT, Van Nostrand Reinhold, p. 37–46.

FRANK, L. A. (1967a): Initial observations of low-energy electrons in the earth's magnetosphere with Ogo 3. J. Geophys. Res., **72**, 185–195.

FRANK, L. A. (1967b): On the extraterrestrial ring current during geomagnetic storms. J. Geophys. Res., **72**, 3753–3767.

FRANK, L. A. (1970): Direct detection of asymmetric increase of extraterrestrial 'ring current' proton intensities in the outer radiation zone. J. Geophys. Res., **75**, 1263–1268.

FRANK, L. A., and K. L. ACKERSON (1971a): Observations of charged particle precipitation into the auroral zone. J. Geophys. Res., **76**, 3612–3643.

FRANK, L. A., and K. L. ACKERSON (1971b): Local-time survey of plasma at low altitudes over the auroral zones. Univ. Iowa Res., Rep., 71-40, August.

FUKUNISHI, H. (1969): Occurrences of sweepers in the evening sector following the onset of magnetospheric substorms. Rep. Ionos. Space Res. Japan, **23**, 21-34.

FUKUSHIMA, N. (1969): Equivalence in ground magnetic effect of Chapman-Vestine's and Birkeland-Alfvén's electric current-systems for polar magnetic storms. Rep. Ionos. Space Res. Japan, **23**, 219-227.

GENDRIN, R. (1968): Pitch-angle diffusion of low energy protons due to gyroresonant interactions with hydromagnetic waves. J. Atmos. Terr. Phys., **30**, 1313-1330.

GENDRIN, R. (1970): Substorm aspects of magnetic pulsations. Space Sci. Rev., **11**, 54-130.

GULYEL'MI, A. V., N. F. MAL'TSEVA, and V. A. TROITSKAYA (1970): On the role of hydromagnetic pulsations of the IPDP type in forming of asymmetric ring current. Paper presented at the International Symposium on Solar-Terrestrial Physics, Moscow.

HEACOCK, R. R. (1967): Two subtypes of type Pi micropulsations. J. Geophys. Res., **72**, 3905-3917.

HEACOCK, R. R. (1968): Large amplitude Pc 1 events at College. J. Geomag. Geoelectr., **20**, 263-269.

HEACOCK, R. R. (1971): The relation of the Pc 1 micropulsation source region to the plasmasphere. J. Geophys. Res., **76**, 100-109.

HIRASAWA, T., and T. NAGATA (1972): Constitution of polar substorm and associated phenomena in the southern polar region. Jap. Antarct. Res. Exped. Sci. Rep., Ser. A, **10**, p. 1-76.

HOFFMAN, R. A., and D. S. EVANS (1968): Field aligned electron bursts at high latitudes observed by Ogo 4. J. Geophys. Res., **73**, 6201-6214.

HONES, E. W., Jr., J. R. ASBRIGE, S. J. BAME, and S. SINGER (1971a): Energy spectra and angular distributions of particles in plasma sheet and their comparison with rocket measurements over the auroral zone. J. Gophys. Res., **76**, 63-87.

HONES, E. W., Jr., S. SINGER, L. J. LANZEROTTI, J. D. PIERSON, and T. J. ROSENBERG (1971b): Magnetospheric substorm of August 25-26, 1967. J. Geophys. Res., **76**, 2977-3009.

IIJIMA, T. (1972): Statistical relationship of the different processes during magnetospheric substorms on the ground and in the distant magnetotail. Rep. Geophys. Res. Lab., Univ. Tokyo, UT-GRL-72-02.

IIJIMA, T., N. FUKUSHIMA, and Y. KAMIDE (1968): Worldwide geomagnetic change preceding the onset of auroral electrojet. Rep. Ionos. Space Res. Japan, **22**, 161-172.

IIJIMA, T., and T. NAGATA (1971): Signatures for substorm development of the growth phase and expansion phase. Rep. Geophys. Res. Lab. Univ. Tokyo, UT-GRL-71-03.

IIJIMA, T., and T. NAGATA (1970): The constitution of magnetosphere storms. Ann. Géophys., **26**, 417-426.

KAMIDE, Y., and N. FUKUSHIMA (1971): Analysis of magnetic storms with DR-indices for equatorial ring current field. Rep. Ionos. Space Res. Japan, **25**, 125-162.

KAMIDE, Y., and N. FUKUSHIMA (1972): Positive geomagnetic bays in evening high-latitudes and their possible connection with partial ring current. Rep. Ionos. Space Res. Japan, **26**, 79-101.

KINDEL, J. M., and C. F. KENNEL (1971): Topside current instabilities. J. Geophys. Res., **76**, 3055-3078.

KISABETH, J. L., and G. ROSTOKER (1971): Development of the polar electrojet during polar magnetic substorms. J. Geophys. Res., **76**, 6815-6828.

KOKUBUN, S. (1971): Polar substorm and interplanetary magnetic field. Planet. Space Sci., **19**. 697-714.

LEZNIAK, T. W., and J. R. WINCKLER (1970): Experimental study of magnetospheric motions and the acceleration of energetic electrons during substorms. J. Geophys. Res., **75**, 7075–7098.

MCPHERRON, R. L. (1970): Growth phase of magnetospheric substorms. J. Geophys. Res., **75**, 5592–5599.

MCPHERRON, R. L., G. K. PARKS, F. V. CORONITI, and S. H. WARD (1968): Studies of the magnetospheric substorm, 2, Correlated micropulsations and electron precipitation occurring during auroral substorms. J. Geophys. Res., **73**, 1697–1713.

MCPHERRON, R. L., C. T. RUSSELL, and M. P. AUBRY (1972): Satellite studies of magnetospheric substorms on August 15, 1968. Note 9. Phenomenological model for substorms. Institute of Geophysics and Planetary Physics, preprint, February.

MEINEL, A. B. (1951): Doppler-shifted auroral hydrogen emission. Astrophys. J., **113**, 50–54.

MENG, C.-I., S.-I. AKASOFU, E. W. HONES, Jr., and K. KAWASAKI (1971): Magnetospheric substorms in the distant magnetotail observed by Imp 3. J. Geophys. Res., **76**, 7584–7594.

MISHIN, V., and A. GRAFE (1971): Models of DP-currents and their dynamics, presented at the IAGA Symposium on Morphology and Physics of Magnetospheric Substorms. IUGG XV General Assembly, Moscow.

MONTBRIAND, L. E. (1971): The proton aurora and auroral substorm. The Radiating Atmosphere, edited by B. M. MCCORMAC, D. Reidel, Dordrecht, Holland, p. 366–373.

OGUTI, T. (1971): Electric coupling between the magnetosphere and the ionosphere as a cause of polar magnetic disturbances and auroral break-up. Cosmic Electrodynamics, **2**, 164–183.

OMHOLT, A. (1957): Photometric observations of rayed and pulsating aurorae. Astrophys. J., **126**, 461–463.

OSSAKOW, S. L. (1968): Anomalous resistivity along lines of force in the magnetosphere. J. Geophys. Res., **73**, 6366–6369.

PFITZER, K. A., and J. R. WINCKLER (1969): Intensity correlations and substorm electron drift effects in the outer radiation belt measured with the Ogo 3 and ATS 1 satellites. J. Geophys. Res., **74**, 5005–5018.

PUDOVKIN, M. I., O. I. SHUMILOV, and S. A. ZAITZEVA (1968): Dynamics of the zone of corpuscular precipitations. Planet. Space Sci., **16**, 881–890.

REES, M. H., and P. C. BENEDICT (1970): The auroral proton oval. J. Geophys. Res., **75**, 4763–4774.

RÈME, H., and J. M. BOSQUED (1971): Evidence near the auroral ionosphere of a parallel electric field deduced from energy and angular distributions of low-energy particles. J. Geophys. Res., **76**, 7683–7693.

RUSSELL, C. T., R. L. MCPHERRON, and P. J. COLEMAN, Jr. (1971): Magnetic field variations in the near geomagnetic tail associated with the weak substorm activity. J. Geophys. Res., **76**, 1823–1829.

SAITO, T. (1969): Geomagnetic pulsations. Space Sci. Rev., **10**, 319–412.

SCHIELD, M. A., and L. A. FRANK (1970): Electron observations between the inner edge of the plasma sheet and the plasmasphere. J. Geophys. Res., **75**, 5401–5414.

SCHIELD, M. A., J. W. FREEMAN, and A. J. DESSLER (1969): A source for field-aligned currents at auroral latitudes. J. Geophys. Res., **74**, 247–256.

SHELLEY, E. G., R. G. JOHNSON, and R. D. SHARP (1971): Plasma sheet convection velocities inferred from electron flux measurements at synchronous altitude. Radio Sci., **6**, 305–313.

STROFFREGEN, W., and H. DERBLOM (1962): Auroral hydrogen emission related to charge separa-

tion in the magnetosphere. Planet. Space Sci., **9**, 711–716.

SWIFT, D. W. (1965): A mechanism for energizing electrons in the magnetosphere. J. Geophys. Res., **70**, 3061–3073.

SWIFT, D. W. (1971): Possible mechanism for formation of the ring current belt. J. Geophys. Res., **76**, 2276–2297.

VASYLIUNAS, V. M. (1968): A survey of low-energy electrons in the evening sector of the magnetosphere with Ogo 1 and Ogo 3. J. Geophys. Res., **73**, 2839–2884.

VASYLIUNAS, V. M. (1969): Mathematical models of magnetospheric convection and its coupling to the ionosphere. Particles and Fields in the Magnetosphere, edited by B. M. MCCORMAC, D. Reidel, Dordrecht, Netherlands, p. 60–71.

VONDRAK, R. R., H. R. ANDERSON, and R. J. SPIGER (1971): Rocket-based measurement of particle fluxes and currents in an auroral arc. J. Geophys. Res., **76**, 7701–7713.

WESTERLUND, L. H. (1969): The auroral electron energy spectrum extended to 45 ev. J. Geophys. Res., **74**, 351–354.

WHALEN, B. A., and I. B. MCDIARMID (1972): Observations of magnetic field-aligned auroral-electron precipitation. J. Geophys. Res., **77**, 191–202.

WIENS, R., and A. VALLANCE JONES (1969): Studies of auroral hydrogen emissions in west-central Canada, 3, Proton and electron auroral ovals. Can. J. Phys., **14**, 1493–1503.

WOLF, R. A. (1970): Some effect of ionospheric conductivity on convective flow of plasma in the magnetosphere. J. Geophys. Res., **75**, 4677–4698.

YEVLASHIN, L. S. (1963): Some patterns of behavior of auroral hydrogen emission. Geomag. Aeronomy, **3**, 405–408.

(*Manuscript received November 2, 1972*)